We are IntechOpen,
the world's leading publisher of
Open Access books
Built by scientists, for scientists

6,900
Open access books available

186,000
International authors and editors

200M
Downloads

154
Countries delivered to

Our authors are among the

TOP 1%
most cited scientists

12.2%
Contributors from top 500 universities

CLARIVATE ANALYTICS
BOOK CITATION INDEX
INDEXED

WEB OF SCIENCE™

Selection of our books indexed in the Book Citation Index
in Web of Science™ Core Collection (BKCI)

Interested in publishing with us?
Contact book.department@intechopen.com

Phase Separations in Mixtures of a Nanoparticle and a Liquid Crystal

Akihiko Matsuyama
Department of Bioscience and Bioinformatics, Kyusyu Institute of Technology
Japan

1. Introduction

Liquid crystal suspensions including various micro- and nano-colloidal particles have recently been received great attention for many practical applications such as nanosensors and devices, etc. When large colloidal particles of micronscale are dispersed in a uniform nematic liquid crystal phase, the colloidal particles disturb a long-range orientational order of the nematic phase. For a strong anchoring between the colloidal surface and a liquid crystal, different defect structures such as hedgehogs or Saturn rings can appear around a single colloidal particle, due to strong director deformations.(Fukuda, 2009; Skarabot et.al., 2008; Stark, 2001) Experiments have also shown two-dimensional crystalline structures of colloidal particles.(Loudet et. al., 2004; Musevic et. al., 2006; Nazarenko et. al., 2001; Pouling et.al., 1997; Yada et. al., 2004; Zapotocky et.al., 1999) On the other hand, under a weak surface anchoring between the colloidal surface and a liquid crystal, the coupling to the orientational elasticity of the liquid crystals tends to expel the colloidal particles and the suspension shows a phase separation into an almost pure nematic phase coexisting with a colloidal rich phase.(Anderson et.al., 2001; Pouling et. al., 1994) Such phase separations induced by a nematic ordering have also been discussed in flexible polymers dispersed in a nematic liquid crystal.(Chiu & Kyu, 1999; Das & Ray, 2005; Dubaut et.al., 1980; Matsuyama & Kato, 1996; Shen & Kyu, 1995)

If the colloidal particles are ~1-10nm in diameter, these "nanoparticles" are too small to distort the nematic director and defects do not form. In this case, the system can show a homogeneous single phase or phase separations,(Anderson et.al., 2001; Anderson & Terentjev, 2001; Caggioni et. al., 2005; Meeker et. al., 2000; Yamamoto & Tanaka, 2001) depending on the interaction between a colloidal particle and a liquid crystal. Although the theoretical progress on the description of a director around colloidal particles with strong anchoring conditions has been noticeable,(Araki & Tanaka, 2004; Fukuda & Yokoyama, 2005; Kuksenok et.al., 1996; Lubensky et. al., 1998; Yamamoto, 2001) little theoretical work exists in phase separations.(Popa-Nita et. al., 2006; Pouling et. al., 1994)

In this chapter, we focus on nanoparticles dispersed in liquid crystals and discuss phase separations and phase behaviors in mixtures of a nanoparticle and a liquid crystal. It is mainly based on authors' original theoretical works obtained within recent years. The nanoparticles have a variety in the shape such as spherical and rodlike. In this chapter, we focus on (1) mixtures of a liquid crystal and a spherical nanoparticle and (2) mixtures of a liquid crystal and a rodlike nanoparticle, such as carbon nanotube. The topics are currently interested in the advanced fields of nanoparticles and fundamental sciences.

When the nanoparticles are dispersed in isotropic solvents, the system may show phase separations, or sodification, between a liquid and a crystalline phase, depending on temperature and concentration, etc. These phase separations are induced by a balance between steric repulsions and attractive dispersion forces. However, the nature of phase separations of nanoparticles dispersed in liquid crystalline solvents is quite difference. The key point is ordering of nanoparticles induced by liquid crystalline ordering. Depending on the interaction between nanoparticles and liquid crystals, we have a variety of phase separations.

The aim of this chapter is to introduce such a new kind of phase separations. We review recent mean field theories to describe phase separations (or phase diagrams) in mixtures of a nanoparticle and a liquid crystal and summarize the variety of phase separations in such nanoparticle dispersions, where liquid crystalline ordering (nematic and smectic A phases) and nanoparticle ordering compete. In Section 2, We discuss spherical nanoparticles dispersed in liquid crystals. Nanotubes dispersed in liquid crystals are discussed in Section 3. The effects of external forces, such as magnetic and electric fields, on the phase behaviors are also discussed in Section 3.

2. Spherical nanoparticles dispersed in liquid crystals

2.1 Ferroelectric nanoparticles dispersed in nematic liquid crystals

Small nanoparticles do not significantly perturb the nematic director. However, it has been recently discovered that ferroelectric nanoparticles can greatly enhance the physical properties of nematic liquid crystals. Recent experimental(Copic et.al., 2007; Li et. al., 2006) and theoretical(Kralj et.al., 2008; Lopatina & Selinger, 2009) studies have shown that low concentrations of ferroelectric nanoparticles ($BaTiO_3$) increase the orientational order of a liquid crystal and increase the nematic-isotropic transition temperature, due to the coupling between the ferroelectric nanoparticle with electric dipole moment and the orientational order of liquid crystals.(Lopatina & Selinger, 2009)
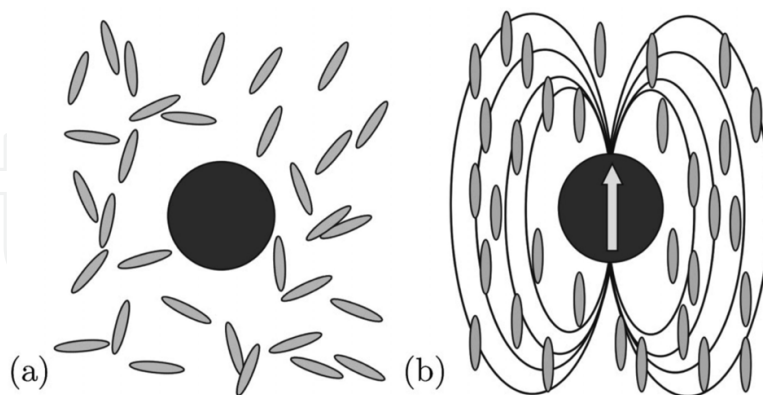

Fig. 1. Nanoparticles dispersed in liquid crystal. (a) Nanoparticle with no electric dipole moment, in an isotropic phase. (b) Ferroelectric particle with dipole moment, which produces an electric field that interacts with orientational order of the nematic phase. Reproduced with permission from (Lopatina & Selinger, 2009) . Copyright 2009 American Physical Society.

As shown in Fig. 1, the orientational distribution of the nanoparticle dipole moment interacts with the orientational order of liquid crystals and stabilizes the nematic phase. The electric

field generated by the nanoparticle interacts with the order parameter of the liquid crystal through the free energy

$$F_{int} = -\frac{\Delta\epsilon\rho_{NP}p^2}{180\pi\epsilon_0\epsilon^2 R^3}S_{LC}S_{NP},$$ (1)

where $\Delta\epsilon$ is the dielectric anisotropy of the aligned liquid crystal, ρ_{NP} is the number density of nanoparticles, and p is the electric dipole moment, S_{LC} (S_{NP}) is the scalar orientational order parameters of the liquid crystals (nanoparticles). This free energy can predict the enhancement in the isotropic-nematic transition temperature and in the response to an applied electric field. The attractive interaction between the liquid crystal and the nanoparticle through the order parameters is important to understand the phase behaviors. The next section we consider the free energy to describe the phase separations.

2.2 Phase ordering in mixtures of a spherical nanoparticle and a liquid crystal

We consider mixtures of a spherical nanoparticle and a liquid crystal. By taking into account the ordering of liquid crystals and nanoparticles, we can expect six possible phases in this mixture. Figure 2 shows the schematically illustrated six phases. The isotropic (I) phase means both liquid crystals and nanoparticles have no positional and orientational order. In the nematic (N) phase, liquid crystals have an orientational order, while nanoparticles have no positional order. Similarly, in the smectic A (A) phase, liquid crystals have a smectic A order, while nanoparticles have no positional order. When the concentration of nanoparticles is high, we may have a crystalline (C) phase of nanoparticles dispersed in an isotopic matrix of liquid crystals. We can also expect a nematic-crystal (NC) phase and a smectic A-crystal (AC) phase, where nanoparticles form a crystalline structure dispersed in a nematic and a smectic A matrix of liquid crystals. To describe these phases, depending on temperature and concentration, we take into account three scalar order parameters: an orientational order parameter for a nematic phase, one-dimensional translational order parameter for a smectic A phase, and a translational order parameter for a crystalline phase of nanoparticles.

2.3 Free energy of mixtures of a spherical nanoparticle and a liquid crystal

We consider a binary mixture of N_c spherical nano-colloidal particles of the diameter R_c and N_r low-molecular weight liquid crystal molecules (liquid crystals) of the length l and the diameter d. The volume of the liquid crystal and that of the nanoparticle are given by $v_r = (\pi/4)d^2l$ and $v_c = (\pi/6)R_c^3$, respectively. Let $\rho_r(\mathbf{u},\mathbf{r})$ and $\rho_c(\mathbf{r})$ be the number density of liquid crystals and colloidal particles with an orientation $\mathbf{u}$ (or its solid angle Ω) at a position $\mathbf{r}$, respectively. The free energy F of the dispersion at the level of second virial approximation is given by(Matsuyama & Hirashima, 2008a; Matsuyama, 2010a)

$$
\begin{aligned}
\beta F/V = &\int \rho_r(\mathbf{r},\mathbf{u})\big[\beta\mu_r^\circ + \ln\rho_r(\mathbf{r},\mathbf{u}) - 1\big]d\mathbf{r}d\Omega \\
&+ \int \rho_c(\mathbf{r})\big[\beta\mu_c^\circ + \ln\rho_c(\mathbf{r}) - 1\big]d\mathbf{r} \\
&+ \frac{1}{2}\iint \rho_r(\mathbf{r},\mathbf{u})\rho_r(\mathbf{r}',\mathbf{u}')\beta_{rr}(\mathbf{r},\mathbf{u};\mathbf{r}',\mathbf{u}')d\mathbf{r}d\Omega d\mathbf{r}'d\Omega', \\
&+ \frac{1}{2}\iint \rho_c(\mathbf{r})\rho_c(\mathbf{r}')\beta_{cc}(\mathbf{r};\mathbf{r}')d\mathbf{r}d\mathbf{r}', \\
&+ \iint \rho_c(\mathbf{r})\rho_r(\mathbf{r}',\mathbf{u}')\beta_{cr}(\mathbf{r};\mathbf{r}',\mathbf{u}')d\mathbf{r}d\mathbf{r}'d\Omega',
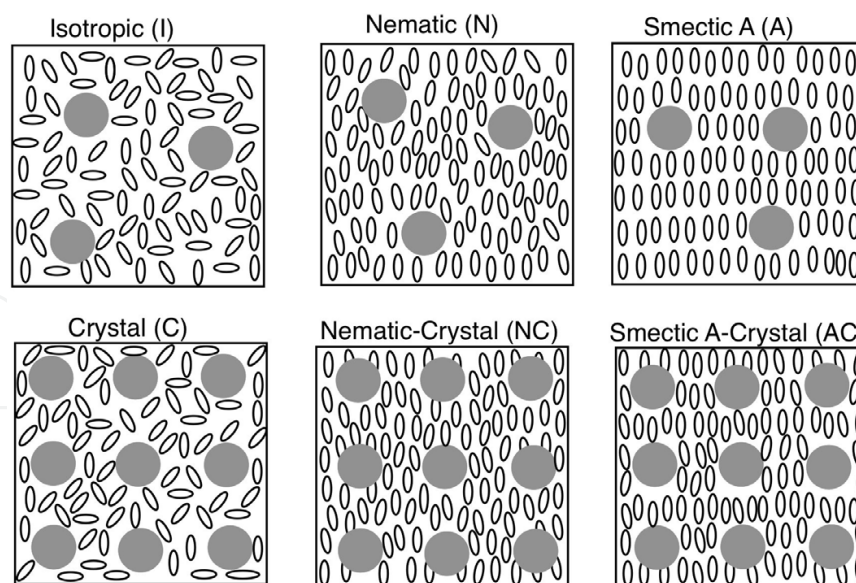\end{aligned}
$$ (2)

Fig. 2. Ordering of nanoparticles dispersed in liquid crystals. We here take into account three scalar order parameters: an orientational order parameter for a nematic phase, one-dimensional translational order parameter for a smectic A phase, and a translational order parameter for a crystalline phase of nanoparticles.

where $d\Omega$ is the solid angle, μ_i° is the standard chemical potential of a particle $i, j (= r, c)$, $\beta \equiv 1/k_B T$; T is the absolute temperature, k_B is the Boltzmann constant, $\beta_{ij} \equiv 1 - \exp[-\beta u_{ij}]$ is the Mayer-Mayer function, and u_{ij} is the interaction energy between two particles i and j.

Let $f_r(\mathbf{r}, \mathbf{u})$ be the distribution function of liquid crystals and then the density can be expressed as

$$\rho_r(\mathbf{r}, \mathbf{u}) = c_r f_r(\mathbf{r}, \mathbf{u}), \tag{3}$$

where $c_r \equiv N_r/V$ is the average number density of liquid crystals. We here consider a nematic and a smectic A phase of liquid crystals and use the decoupled approximation(Kventsel et.al., 1985) for the distribution function:

$$f_r(\mathbf{r}, \mathbf{u}) = f_r(\tilde{z}_r) f_r(\mathbf{u}), \tag{4}$$

where $\tilde{z}_r \equiv z/l$, l is the average distance between smectic layers, $f_r(\tilde{z}_r)$ is the translational distribution function of liquid crystals for a smectic A phase, and $f_r(\mathbf{u})$ is the orientational distribution function of liquid crystals for a nematic phase. Similarly, using the translational distribution function $f_c(\mathbf{r})$ of nanoparticles, the density of nanoparticles can be expressed as

$$\rho_c(\mathbf{r}) = c_c f_c(\mathbf{r}), \tag{5}$$

where $c_c \equiv N_c/V$ is the average density of nanoparticles. The total number N_r of liquid crystals and N_c of nanoparticles must be conserved and then we have the normalization conditions:

$$\iint \rho_r(\mathbf{r}, \mathbf{u}) d\mathbf{r} d\Omega = N_r/V, \tag{6}$$

and

$$\int \rho_c(\mathbf{r}) d\mathbf{r} = N_c/V. \tag{7}$$

The orientational order parameter S of a nematic phase is given by(Maier & Saupe, 1958)

$$S = \int P_2(\cos\theta) f_r(\theta) d\Omega, \tag{8}$$

where $P_2(\cos\theta) \equiv 3(\cos^2\theta - 1/3)/2$. The translational order parameter σ_s of a smectic A phase is given by(McMillan, 1971)

$$\sigma_s = \int_0^1 \cos(2\pi\tilde{z}_r) f_r(\tilde{z}_r) d\tilde{z}_r. \tag{9}$$

In the McMillan's model,(McMillan, 1971) the order parameter for the smectic A phase is given by $\langle P_2(\cos(\theta))\cos(2\pi\tilde{z}_r)\rangle$. In Eq. (4), we have used the decoupled approximation: $\langle P_2(\cos(\theta))\cos(2\pi\tilde{z}_r)\rangle = S\sigma_s$. It has been reported that the decoupled model for the smectic A phase is in quantitative agreement with the original McMillan's theory.(Kventsel et.al., 1985) In the decoupled model, the smectic A phase is defined by $S \neq 0$ and $\sigma_s > 0$.

For a crystalline phase, we here consider a face-centered cubic (fcc) structure of nanoparticles for example. The translational order parameter for a fcc crystalline phase can be calculated by(Kirkwood & Monroe, 1941)

$$\sigma_f = \int_0^1\int_0^1\int_0^1 \cos(2\pi\tilde{x})\cos(2\pi\tilde{y})\cos(2\pi\tilde{z}) f_c(\tilde{\mathbf{r}}) d\tilde{\mathbf{r}}, \tag{10}$$

where L is the lattice size of a fcc crystal and we define $\tilde{x} \equiv x/L$, $\tilde{y} \equiv y/L$, $\tilde{z} \equiv z/L$, and $d\tilde{\mathbf{r}} \equiv d\tilde{x}d\tilde{y}d\tilde{z}$. It is possible to consider the other crystalline structure such as a body-centered cubic and a simple cubic, etc.(Matsuyama, 2006a;b)

When the interaction between liquid crystals is a short-range attractive interaction, the anisotropic part of the interaction can be given by Fourier components of the potential:(McMillan, 1971)

$$\beta_{rr} \simeq -(v_r l/d)\nu S\big(1 + \gamma\sigma_s\cos(2\pi z/l)\big)P_2(\cos\theta) \tag{11}$$

where we have retained the lowest order of the Fourier components. The $\nu(\equiv U_a/k_BT)$ is the orientational dependent (Maier-Saupe) interaction parameter between liquid crystals(Maier & Saupe, 1958) and the γ shows the dimensionless interaction of a smectic phase(Matsuyama & Kato, 1998; McMillan, 1971). According to the McMillan theory, the parameter γ is given by $\gamma = 2\exp[-(r_0/l)^2]$, which can vary between 0 and 2, and increases with increasing the chain length of alkyl end-chains of a liquid crystal. The smectic condensation is more favored for larger values of γ. For the anisotropic interaction between nanoparticles in a fcc crystalline phase, the anisotropic part of the interaction can be given by expanding β_{cc} at the lowest order of the Fourier components:(Kirkwood & Monroe, 1941)

$$\beta_{cc} \simeq -(v_c R_c/d)g\sigma_f\cos(2\pi\tilde{x})\cos(2\pi\tilde{y})\cos(2\pi\tilde{z}), \tag{12}$$

where the coefficient β_{cc} is proportional to the total surface area $(v_c R_c)$ of two particles. The parameter $g(\equiv -\beta f_0)$ is the dimensionless interaction parameter between nanoparticles, where the interaction energy f_0 consists of an entropic and enthalpic terms. In this paper, we only consider short-range interactions between particles. The long-range interaction, due to

the presence of surface charges, is not taken into account. Similarly to Eq. (11), the anisotropic interaction between a nanoparticle and a liquid crystal in a nematic and a smectic$A$ phase is given by

$$\beta_{cr} \simeq \frac{1}{2}(v_c l / R_c)\omega S\big(1 + \omega_1 \sigma_s \cos(2\pi z/l)\big)P_2(\cos\theta), \tag{13}$$

where β_{cr} is proportional to the surface area (v_c/R_c) of a nanoparticle(Stark, 1999). The $\omega \equiv w_0/k_B T$ shows the dimensionless interaction parameter between a liquid crystal and a particle surface. When $\omega > 0$, or repulsive interaction between a liquid crystal and a nanoparticle, doping nanoparticles disturb the orientational ordering of liquid crystals, or the orientational elasticity of the liquid crystals tends to expel the particles to be lower the elastic free energy of a nematic phase(Pouling et. al., 1994). In the mean field level, the elastic distortion cost of a director is taken into account in the order of ωS^2. The negative values of $\omega(< 0)$ indicate the attractive interactions between a liquid crystal and a nanoparticle and the particles tend to disperse into a liquid crystalline matrix as indicated in Fig. 1. The last term $\omega_1(> 0)$ is the coupling between a smectic liquid crystal and a colloidal surface.

We here assume the system is incompressible. Let $\phi_r = v_r N_r / V$ and $\phi_c = v_c N_c / V$ be the volume fraction of a liquid crystal and a nano-colloidal particle, respectively. Using the axial ratio $n_r (\equiv l/d)$ of a liquid crystal and $n_c \equiv R_c/d$, the volume of a particle is given by $v_r = a^3 n_r$ and $v_r \simeq (a n_c)^3$, where we define $a^3 \equiv (\pi/4)d^3$. To describe phase behaviors of the incompressible blends, we calculate the free energy of mixing for the binary mixtures of a liquid crystal and a nanoparticle:

$$\Delta F = F(N_c, N_r) - F(N_c, 0) - F(0, N_r), \tag{14}$$

where the $F(N_c, 0)$ and $F(0, N_r)$ are the reference free energy of the pure nanoparticles and the pure liquid crystal in an isotropic phase, respectively. Substituting Eqs. (11)-(13) into (14), the mixing free energy is given by

$$\Delta F = F_{mix} + F_c + F_{nem} + F_{sm} + F_{anc}, \tag{15}$$

where the each term is given as following.

The first term in Eq. (15) shows the free energy for mixing of colloids and liquid crystals in the isotropic phase:

$$a^3 \beta F_{mix}/V = \frac{\phi_r}{n_r}\ln\phi_p + \frac{\phi_c}{n_c^3}\ln\phi_c + \chi\eta_c\phi_r, \tag{16}$$

where the first and the second terms in Eq. (16) correspond to the entropy of isotropic mixing for liquid crystals and colloidal particles, respectively. We here have added the third term which shows the isotropic interaction parameter $\chi \equiv U_0/k_B T$ related to the dispersion force between a colloidal particle and a liquid crystal, where U_0 is the interaction energy between a colloid and a liquid crystal in an isotropic state. A positive χ denotes that the colloid-liquid crystal contacts are less favored compared with the colloid-colloid and liquid crystal-liquid crystal contacts. This interaction parameter is well known as the Flory-Huggins parameter in polymer solutions.(Flory, 1953) For a colloidal particle, its surface only can interact with the surrounding solvents and so the probability for the colloid-liquid crystal contact is proportional to $\eta_c\phi_r$, where the η_c is the surface fraction of colloidal particles and is

given by

$$\eta_c \equiv \frac{a^2 n_c^3 N_c}{a^2 (n_r N_r + n_c^3 N_c)} = \frac{\phi_c}{n_c}. \tag{17}$$

Then the dispersion interaction due to the mixing is given by $\chi \eta_c \phi_r$. On increasing the diameter n_c of a colloid, the interaction term decreases with a fixed ϕ_c. Eq. (16) corresponds to the extended Flory-Huggins free energy for the isotropic mixtures of a liquid crystal, whose the number of segments is n_r, and a colloidal particle, whose the number of segments is n_c^3. The second term in Eq. (15) shows the free energy for a crystalline ordering of colloidal particles:

$$a^3 \beta F_c / V = \frac{\phi_c}{n_c^3} \int_0^1 \int_0^1 \int_0^1 f(\tilde{\mathbf{r}}) \ln f(\tilde{\mathbf{r}}) d\tilde{\mathbf{r}}$$

$$- \frac{1}{2} g \eta_c^2 \sigma_f^2, \tag{18}$$

where the first term in Eq. (18) shows the entropy loss due to the crystalline ordering. When the colloidal particles have no positional order, we have the distribution function $f(\tilde{\mathbf{r}}) = 1$ and the free energy (F_c) becomes zero. The third term in Eq. (15) shows the free energy for nematic ordering of liquid crystals:

$$a^3 \beta F_{nem} / V = \frac{\phi_r}{n_r} \int f_r(\theta) \ln 4\pi f_r(\theta) d\Omega$$

$$- \frac{1}{2} \nu \phi_r^2 S^2, \tag{19}$$

where the first term in Eq. (19) shows the entropy change due to the nematic ordering. The forth term in Eq. (15) shows the free energy for smectic A ordering of liquid crystals:

$$a^3 \beta F_{sm} / V = \frac{\phi_r}{n_r} \int_0^1 f_r(\tilde{z}_r) \ln f_r(\tilde{z}_r) d\tilde{z}_r$$

$$- \frac{1}{2} \nu \gamma \phi_r^2 (S \sigma_s)^2. \tag{20}$$

The last term in Eq. (15) shows the anchoring interaction between a colloidal surface and a liquid crystal:

$$a^3 \beta F_{anc} / V = \frac{\omega}{2} \eta_c \phi_r \left(S^2 + \omega_1 (S \sigma_s)^2 \right). \tag{21}$$

In a thermal equilibrium state, the distribution functions of nanoparticles and liquid crystals are determined by minimizing the free energy (15) with respect to these functions: $(\delta F / \delta f_c(\tilde{\mathbf{r}}))_{\{f_r(\theta), f_r(\tilde{z}_r)\}} = 0$, $(\delta F / \delta f_r(\theta))_{\{f_c(\tilde{\mathbf{r}}), f_r(\tilde{z}_r)\}} = 0$, and $(\delta F / \delta f_z(\tilde{z}_r))_{\{f_c(\tilde{\mathbf{r}}), f_r(\theta)\}} = 0$. The order parameters S, σ_s, and σ_f can be determined by Eqs. (8), (9), and (10), respectively. Using these distribution functions and order parameters, we can calculate the free energy of our systems. The chemical potentials of a nanoparticle and a liquid crystal can be obtained from this free energy.

2.4 Phase transitions in nanoparticle/liquid crystal mixtures

In a mixture of a nanoparticle and a liquid crystal, we have some phase transitions, depending on temperature and concentration(Matsuyama, 2009).

One is the nematic-isotropic phase transition of this mixture. The nematic-isotropic transition (NIT) temperature is given by

$$\tau_{NI} = T/T_{NI}^{\circ} = 1 - (1 + \alpha_a/n_c)\phi_c, \tag{22}$$

where T_{NI}° shows the NIT temperature of a pure liquid crystal. We here define the ratio α_a between the anchoring strength (w) and the nematic interaction (v):

$$\alpha_a \equiv w/v. \tag{23}$$

The value of α_a shows the anchoring strength. The negative sign represents attractive interaction between a nanoparticle and a liquid crystal and thus the nanoparticles tend to disperse in a liquid crystalline matrix. On the other hand, the positive sign represents the repulsive interaction and the liquid crystals tend to expel the nanoparticles. The slope of the NIT line on the $T - \phi_c$ plane depends on the value of α_a/n_c.

The smectic A−nematic phase transition (ANT) is given by

$$\tau_{AN} = T/T_{NI}^{\circ} = 2.27\gamma\big[1 - (1 + \frac{\omega_1\alpha_a}{n_c\gamma})\phi_c\big]S^2. \tag{24}$$

Since $\gamma > 0$ and $\omega_1 > 0$, the ANT temperature depends on the sign of α_a. For larger negative values of α_a, the ANT temperature increases with increasing ϕ_c. It can also be obtained the direct phase transition from an isotropic to a smectic A phase(Matsuyama, 2009).

We also have the isotropic fluid-crystal phase transition (ICT). The ICT temperature is given by

$$\tau_{IC} = T/T_{NI}^{\circ} = \frac{0.58\alpha_c n_c \phi_c}{n_r(1 - \phi_c/\phi_c^*)}, \tag{25}$$

where

$$\alpha_c \equiv \beta|e_0|/v, \tag{26}$$

shows the strength of the attractive interaction between nanoparticles compared to the nematic interaction parameter v. When $\tau < \tau_{IC}$ the crystalline phase is stable. The ICT temperature increases with increasing ϕ_c and diverges at ϕ_c^*. This corresponds to the entropically driven-liquid-solid transition for hard spherical particles due to the excluded volume interactions.(Alder & Wainwright, 1957; Cates & Evans, 2000)

Figure 3(a) shows the first-order phase transition lines for NIT (red dotted-line, Eq. (22)), ANT (blue dotted-line, Eq. (24)), and ICT (black dotted-line, Eq. (25)) on the reduced temperature (T/T_{NI}°)−concentration (ϕ_c) plane. We set $n_c = 3$, $n_r = 2$, α_c=0.1, $\alpha_a = -2.5$, $\alpha_n(\equiv v/\chi)$=5, $\gamma = 0.87$, $\omega_1 = 1$ for a typical example. When $\phi_c = 0$, or pure liquid crystals, the ANT appears at $T/T_{NI}^{\circ} \approx 0.938$, which is consistent with the result of the MacMillan theory. At high temperatures and low concentrations, we have the isotropic (I) liquid phase. On decreasing temperature, the N phase appears, where nanoparticles are in an isotropic liquid state but liquid crystals are in a nematic state. Further decreasing temperature the smectic A phase
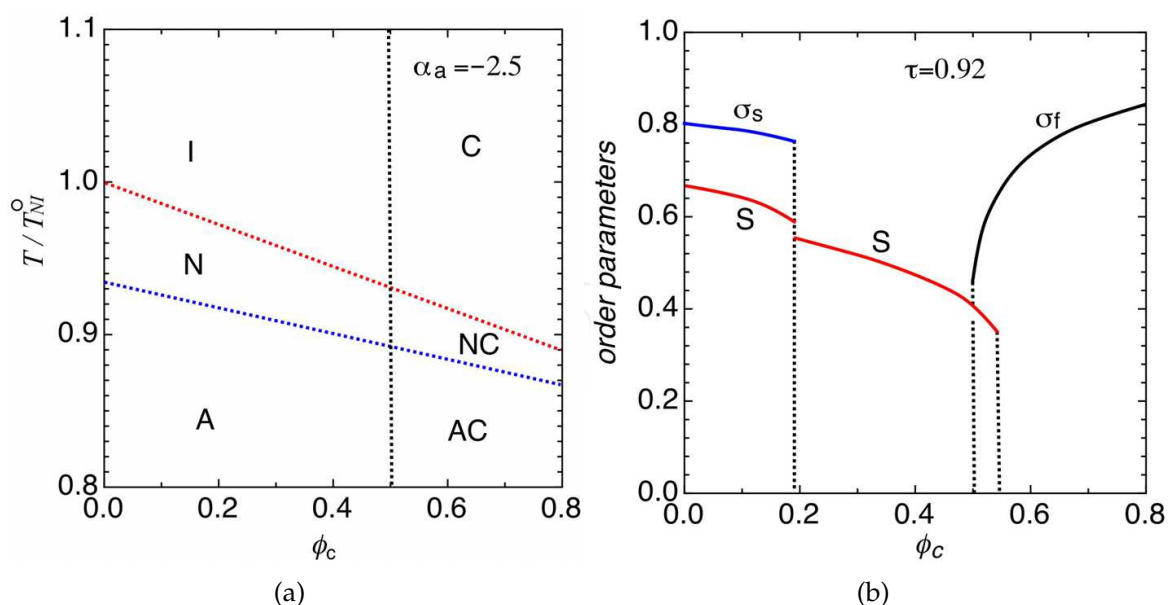
Fig. 3. (a) The first-order phase transition lines (the red dotted-line for NIT (Eq. (22)), the blue dotted-line for ANT (Eq. (24)), and the black dotted-line for ICT (Eq. (25))) on the reduced temperature (T/T_{NI}°)−concentration (ϕ_c) plane. (b) Order parameters plotted against the volume fraction of colloidal particles at T/T_{NI}°=0.92 in Fig. 3(a).

appears, where nanoparticles are in an isotropic liquid state but liquid crystals are in a smectic A phase. At high temperatures and high concentrations, we have the crystalline (C) phase of colloidal particles. On decreasing temperature, the NC phase appears, where colloidal particles are in a crystalline state and liquid crystals are in a nematic state. Further decreasing temperature the AC phase appears, where colloidal particles are in a crystalline state and liquid crystals are in a smectic A phase. The slope of the transition lines depends on the anchoring energy (α_a) as discussed in Eq. (23). For larger negative values of α_a, the slopes of the NIT and ANT lines become positive on the temperature-concentration plane and the nematic and smectic A phase appear at higher temperatures.

Figure 3(b) shows order parameters plotted against the volume fraction ϕ_c at $T/T_{NI}^{\circ} = 0.92$ in Fig. 3(a). On increasing ϕ_c, we find the first-order phase transition from the smectic A to nematic (N) phase at $\phi_c \simeq 0.2$, where the order parameters S and σ_s jump. At $\phi_c \simeq 0.5$, the first-order phase transition from the N to NC phase appears. Further increasing ϕ_c the first-order phase transition from the NC to C phase appears at $\phi_c \simeq 0.55$.

2.5 Phase diagrams of nanoparticle/liquid crystal mixtures

In this subsection we show some phase diagrams calculated from the free energy(15). The coexistence curve (binodal) can be obtained by solving the two-phase coexistence conditions: the chemical potentials of each component are equal in each phase. This binodal curve can also be derived by a double tangent method where the equilibrium volume fractions fall on the same tangent line to the free energy curve.

Figure 4 shows the phase diagrams for $n_r = 2$, $n_c = 3$, $\omega_1 = 1$, $\alpha_c = 0.1$, $\alpha_n = 5$, and $\gamma = 0.87$ for an example. The value of α_a is changed: (a) $\alpha_a = 1$; (b) $\alpha_a = -2$; (c) $\alpha_a = -3.5$.

We here discuss the effects of the anchoring strength α_a on the phase behavior. The negative values of α_a mean that the nanoparticles prefer to disperse into liquid crystalline phases. The solid curve shows the binodal curve. The red, blue, and black dotted lines show the NIT, ANT, and ICT line, respectively (see Fig. 3(a)). When $\phi_c = 0$, the smectic A phase appears at $T/T_{NI}^\circ = 0.94$. When $\alpha_a = 1$ [Fig. 4(a)], we have the broad nematic-isotropic ($N + I$) phase separation between $1 > T/T_{NI}^\circ > 0.94$. Below $T/T_{NI}^\circ < 0.94$, we have the smectic A-isotropic ($A + I$) phase separation. The nematic and smectic A phase at the lower concentrations consist of almost pure liquid crystals. The triple point ($A + I + C$) appears at $T/T_{NI}^\circ = 0.89$, where the smectic A, isotropic, and crystalline phases can simultaneously coexist. Below the triple point, we have the two-phase coexistence ($A + C$) between a smectic A and a crystalline phase. Above the triple point, two-phase coexistence ($I + C$) between an isotropic and a crystalline phase appears.

On decreasing the anchoring parameter α_a the phase behavior is drastically changed. When $\alpha_a = -2$ [Fig. 4(b)], the NIT (Eq. (22)) and ANT (Eq. (24)) lines shift to higher concentrations and the stable single N and A phases appear at low concentrations of nanoparticles. Two tie lines with arrows show the three-phase coexistence: $A + N + I$ and $A + I + C$. Above the triple point $A + N + I$, we have two-phase coexistence $A + N$ and $N + I$. Below the triple point $A + N + I$, we have A+I phase separation. Below the triple point $A + I + C$, we have the broad A+C phase separation.

Further decreasing α_a, Fig. 4(c), the nematic and smectic A ordering are promoted by adding nanoparticles and the NIT and ANT lines shift to higher temperatures. This increase of the NIT and ANT temperature indicates the attractive interactions between a liquid crystal and a colloidal particle. For example, it has been observed that doping low concentrations of ferroelectric $BaTiO_3$ nanoparticles into liquid crystals increases NIT temperature(Li et. al., 2006a). In this case, ferroelectric nanoparticle with electric dipole moment, which produces an electric field, interacts with orientational order of liquid crystals and stabilizes the nematic phase.(Lopatina & Selinger, 2009) This corresponds to negative anchoring energy in our model. We also have three triple points: $I + C + NC$, $N + NC + AC$, and $N + A + AC$. Above the $I + C + NC$ triple point, we have the $I + C$ and $C + NC$ phase separations. Below the $I + C + NC$ triple point, the $I + NC$ and $NC + AC$ phase separations appear. Below the triple point $N + NC + AC$, we have the $I + N$ and $N + AC$ phase separations. Below the triple point $N + A + AC$ we have $N + A$ and $A + AC$ phase separations. The anchoring energy between liquid crystals and nanoparticles becomes an important parameter to derive a stable N, A, NC, and AC phases in the mixture of nanoparticles and liquid crystals.

Anderson et al. have observed the phase ordering of colloidal (PMMA) particles dispersed in a liquid crystal, 5CB or MBBA.(Anderson et.al., 2001) Particles are covered with chemically grafted short chains, making hairy particles. In a nematic phase, the grafted chains tend to provide a homeotropic (radial) director anchoring. In an isotropic liquid, these particles behave like almost hard spheres and so the $I + C$ phase separation takes place at high concentrations of the colloidal particles. Such $I + C$ phase separation, calculated in Fig. 4, has been observed in colloidal dispersions(Pusey & van Megen, 1986) and protein solutions(Tanaka et. al, 2020). At dilute concentrations of the colloidal particles, Anderson et al. observed a decrease in the NIT temperature T_{NI} as a function of ϕ_c, which follows a linear law. This is consistent with Eq. (22). The N+I and N+C phase separations have also been reported in Latex polyballs suspended in an isotropic micellar solution which exhibits
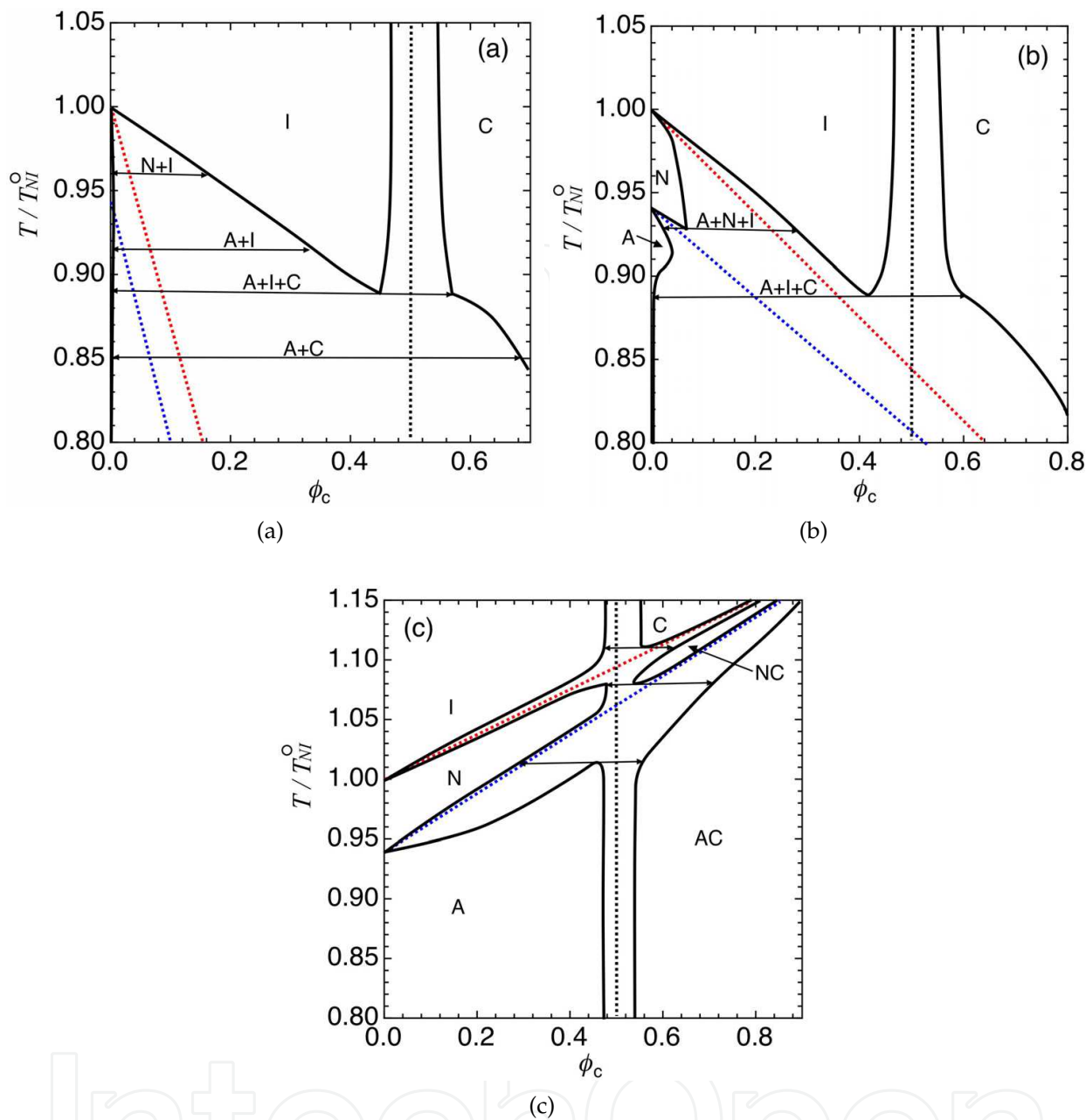
Fig. 4. Phase diagrams for $\alpha_c = 0.1$, $\alpha_n = 5$, $\gamma = 0.87$. The value of α_a is changed: (a) $\alpha_a = 1$; (b) $\alpha_a = -2$; (c) $\alpha_a = -3.5$.

a nematic phase at low temperature.(Pouling et. al., 1994) The observed phase diagram are qualitatively consistent with Fig. 4(a).

The binodal lines calculated at high concentrations of nanoparticles may not be experimentally observed because of high viscosity, however, it is important to understand the phase ordering kinetics(Matsuyama et .al., 2000; Matsuyama, 2008b). The cooperative phenomena between liquid crystalline ordering and crystalline ordering induce a variety of phase separations.

3. Nanotubes dispersed in liquid crystals

Since the discovery of carbon nanotubes (CNTs)(Iijima, 1991), extensive studies of physical and chemical properties of CNTs have been received great attention for many practical applications such as nano-sensors and devices. Windle's group first reported the nematic liquid crystalline behavior of an aqueous suspension of CNTs above a certain concentration and the isotropic-nematic phase separations.(Shaffer & Windle, 1999; Song et. al., 2003). Long nanotubes segregate preferentially to the liquid crystalline phase, whereas shorter nanotubes segregate preferentially to the isotropic phase(Zhang et.al., 2006). Recently such nanotubes as liquid crystalline materials become an important to be used in biological applications such as biosensors, biology imaging, artificial muscles, gene delivery, etc(Woltman et al., 2007).

In order to prepare CNT dispersions, strong van der Waals attractions between nanotubes must be screen out. To do this, the surface of nanotubes can be modified by acid oxidation, acid protonation, polymer or surfactant wrapping, etc.(Zhang & Kumar, 2008). For example, a water-soluble polymer, biopolymers such as DNA, and surfactant molecules have been used to wrap CNT and to increase the dispersibility in water(Badaire et. al., 2005). The polymer-wrapped nanotubes can be dispersed in a solvent with a considerable concentration. The excluded volume and electro-static repulsion between polymers can overcome the intermolecular van der Waals attractions and therefore the polymer-wrapped CNT can be dispersed in water. Thus it is possible to change the strength of the intermolecular interaction between nanotubes by using polymer-wrapping and negative or positive charging of nanotube surface, etc.

Alignment of such CNTs, or rigid-rodlike polymers (rods), with the aid of low molecular-weight-liquid crystalline molecules is an alternative approach. Indeed thermotropic(Basu & Iannacchione, 2008; Dierking et.al., 2005; Jayalakshmi & Prasad, 2009; Lynch & Patrick, 2002; Russell et.al., 2006) as well as lyotropic nematic liquid crystals(Courty et.al., 2003; Lagerwall et. al., 2007; Schymura et. al., 2009; Weiss et. al., 2006) have been applied as nematic solvents for the alignment of nanotubes. Anisotropic interactions between the nanotube and liquid crystal drastically change the alignments and physical properties of the mixtures. Duran et.al. have observed the nematic-isotopic phase transition temperature (T_{NI}) is enhanced by the incorporation of a multi-wall CNT within a small composition gap(Duran et.al., 2005).

In this section, we discuss phase separations in binary mixtures of a low molecular-weight-liquid crystal and a nanotube, such as CNT. We discuss uniaxial and biaxial nematic phases.

3.1 Nematic phases in mixtures of a nanotubes and a liquid crystal

We here consider the effect of the anisotropic interaction between a nanotube and a liquid crystal and that between rods.(Matsuyama, 2010) Depending on the interaction between a nanotube and a liquid crystal, we can expect various nematic phases. Figure 5 schematically shows the four nematic phases, defined by using the orientational order parameter (S_1) of a liquid crystal and that (S_2) of a nanotube. When the orientational order parameter of one component is positive, determining a nematic director, and the orientational order parameter of the second component is negative, we have planer nematic phase, where the second
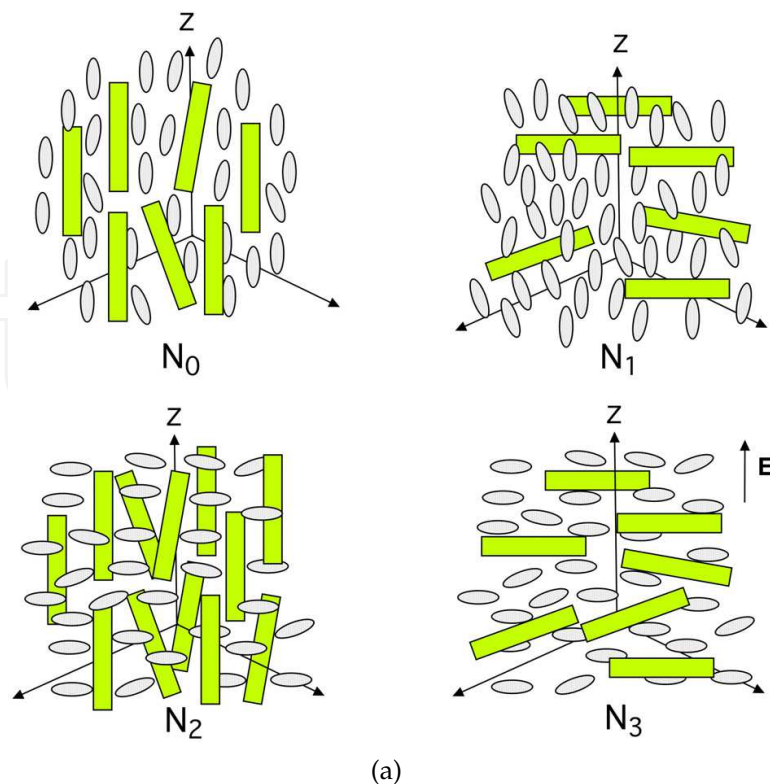
(a)

Fig. 5. Schematically illustrated four possible nematic phases. Four nematic phases are defined using the orientational order parameter S_1 of the liquid crystal and that S_2 of the nanotube: the nematic N_0 phase with $S_1 > 0$ and $S_2 > 0$, the nematic N_1 phase with $S_1 > 0$ and $S_2 < 0$, and the nematic N_2 phase with $S_1 < 0$ and $S_2 > 0$. When an external field (**E**) is applied along to the z axis for the particles of the dielectric anisotropy $\Delta \epsilon_1 < 0$ and $\Delta \epsilon_2 < 0$, the N_3 phase with $S_1 < 0$ and $S_2 < 0$ can appear: the nanotubes and liquid crystals are randomly oriented on the plane perpendicular to the direction of the external field.

component is randomly oriented within in the perpendicular plane to the nematic director. The nematic N_0 phase shows the nanotube and the liquid crystal are parallel to each other: $S_1 > 0$ and $S_2 > 0$. The nematic N_1 phase is defined as that the nanotube and the liquid crystal are perpendicular with each other: $S_1 > 0$ and $S_2 < 0$. In this phase, the nematic director (z axis) can be defined by the orientational direction of the liquid crystals. These perpendicular alignments can be obtained by modifying the surface of a nanotube, or CNT, with polymers or surfactants. The nematic N_2 phase is defined as the nanotube and the LC are perpendicular each other with $S_1 < 0$ and $S_2 > 0$. In this phase, the nematic director (z axis) can be defined by the orientational direction of the nanotube. Biaxial nematic phases are discussed in Section 3.3. When an external field (**E**) is applied along to the z axis for the particles of the dielectric anisotropy $\Delta \epsilon_1 < 0$ and $\Delta \epsilon_2 < 0$, the N_3 phase with $S_1 < 0$ and $S_2 < 0$ may appear, where the nanotubes and liquid crystals are randomly oriented on the plane perpendicular to the direction (z axis) of the external field.

3.2 Free energy of nanotube/liquid crystal mixtures

We consider a binary mixture of a liquid crystal of the length L_1 and the diameter D_1 and and a nanotube of the length L_2 and the diameter D_2: $L_1 < L_2$. The volume of the liquid crystal and

that of the nanotube is given by $v_1 = (\pi/4)D_1^2 L_1$ and $v_2 = (\pi/4)D_2^2 L_2$, respectively. We here assume $D \equiv (D_1 = D_2)$. Let $\rho_1(\mathbf{r}, \mathbf{u})$ and $\rho_2(\mathbf{r}, \mathbf{u})$ be the number density of the liquid crystals and the nanotubes with an orientation $\mathbf{u}$ (or its solid angle Ω) at a position $\mathbf{r}$, respectively. The free energy F of the dispersion at the level of second virial approximation is given by Eq. (2). The volume fraction of liquid crystals is given by $\phi_1 = v_1 \rho_1$ and tat of nanotubes $\phi_2 = v_2 \rho_2$. As discussed in Eq. (14), we here consider the incompressible fluids: $\phi_1 + \phi_2 = 1$.

Consider a uniaxial nematic phase, which is spatially uniform but nonuniform for orientation. Let $f_i(\mathbf{u})$ be the distribution function of the particle $i(= 1, 2)$ and then the density can be expressed as

$$\rho_i(\mathbf{r}, \mathbf{u}) = c_i f_i(\mathbf{u}), \qquad (27)$$

where $c_i \equiv N_i/V$ is the average number density of the particle i . The total number N_1 of the liquid crystals and N_2 of the nanoparticles must be conserved and then we have the normalization conditions:

$$\int \rho_i(\mathbf{r}, \mathbf{u}) d\mathbf{r} d\Omega = N_i/V, \qquad (28)$$

where $d\Omega = 2\pi \sin\theta d\theta$ for a uniaxial nematic phase.

For the interaction between liquid crystals in Eq. (2), we take the attractive (Maier-Saupe) interaction:

$$\beta_{11} = -\nu_1 v_1 P_2(\cos\theta) P_2(\cos\theta'), \qquad (29)$$

where $\nu_1(\equiv U_1/k_B T > 0)$ and U_0 is the anisotropic attractive (Maier-Saupe) interaction between liquid crystals(Brochard et.al., 1984; Maier & Saupe, 1958). (The subscript symbols c and r in Eq. (2) are changed to 1 and 2, respectively.)   For the interaction between nanotubes, we here take into account both the attractive interaction and excluded volume one:(Matsuyama & Kato, 1996)

$$\beta_{22} = 2L^2 D|\mathbf{u} \times \mathbf{u}'| - \nu_2 v_2 P_2(\cos\theta) P_2(\cos\theta'), \qquad (30)$$

where the first term is the excluded volume interaction between nanotubes, or rods,(Onsager, 1949) and the $\nu_2(\equiv U_2/k_B T > 0)$ is the attractive (Maier-Saupe) interaction between nanotubes. The interaction between a liquid crystal and a nanoparticle is given by

$$\beta_{12} = -\nu_{12} v_{12} P_2(\cos\theta) P_2(\cos\theta'), \qquad (31)$$

where the anisotropic interaction $\nu_{12}(\equiv U_{12}/k_B T)$ between a liquid crystal and a rod can be positive or negative value. We here assume that the excluded volume interaction of a liquid crystal can be negligible because the length of liquid crystal is short. The volume $v_{12} = (\pi/4)L_1 L_2 D$ is the average excluded volume between a rod and a liquid crystal in an isotropic phase, Using Eqs. (29), (30), and (31), we can obtain the mixing free energy (15) for nanotube/liquid crystal mixtures. We here define an interaction parameter between a nanotube and a liquid crystal:

$$c_{12} = v_{12}/v_1, \qquad (32)$$

which becomes an important parameter in the phase behavior.

3.3 Phase diagrams of nanotube/liquid crystal mixtures

In this subsection, we show some phase diagrams calculated from the free energy(Matsuyama, 2010).
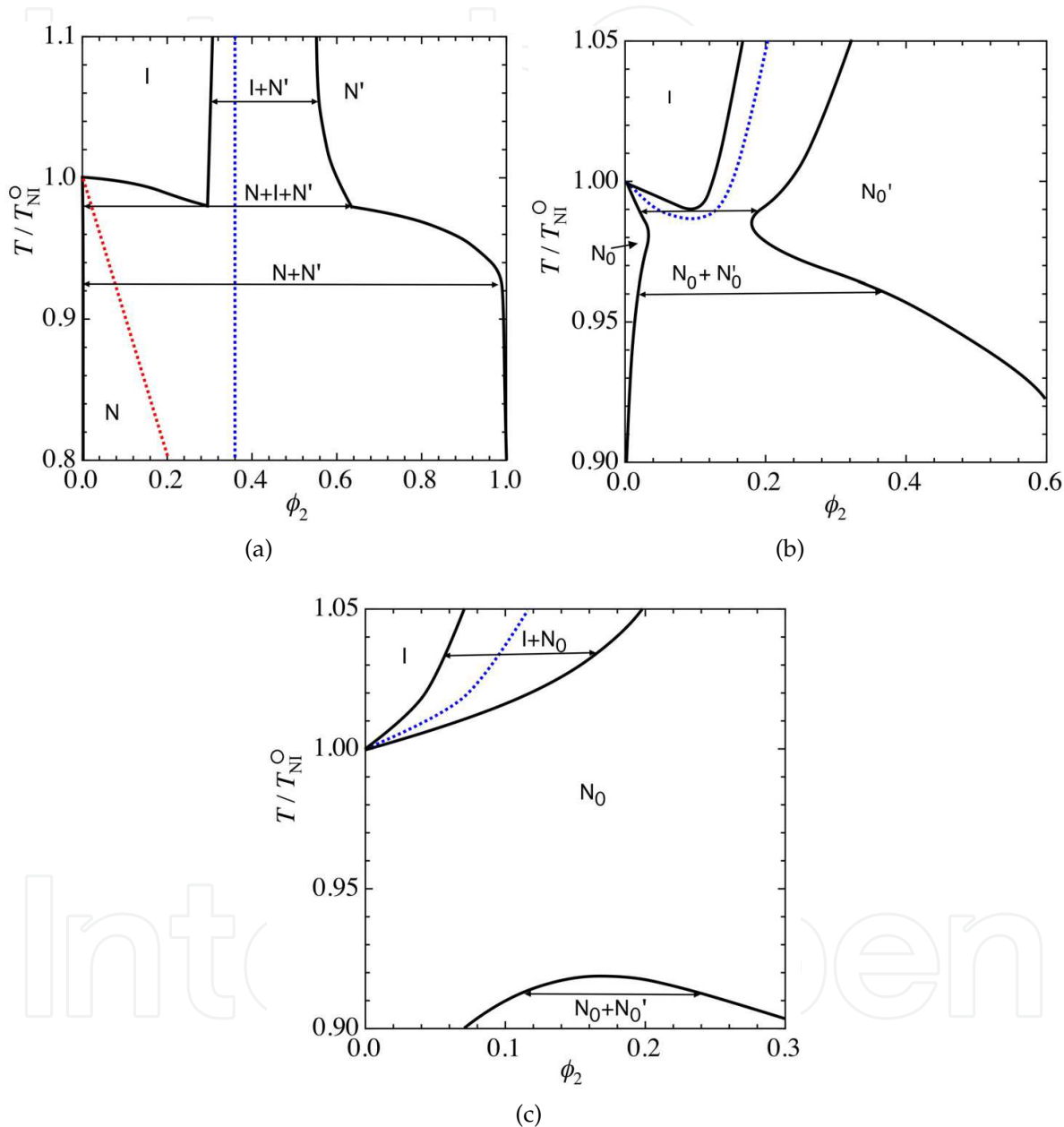
3.3.1 Uniaxial nematic N_0 phase

Fig. 6. Phase diagrams for c_{12}=0 (a), c_{12}=0.3 (b), and c_{12}=0.4(c) with $n_1 = 2$ and $n_2 = 10$.

We first show the phase diagram for $c_{12} = 0$ (see Fig. 6(a)), where the excluded volume interaction between nanotubes only prevails. The solid curve shows the binodal. The red and blue dotted lines show the first-order NIT line of a liquid crystal and that of a nanotube, respectively. Above $T/T_{NI}^\circ = 1$, the NIT of nanotubes takes place with increasing the concentration of the nanotube due to the excluded volume interaction between nanotubes,

and we have the isotropic (I)-nematic (N) phase separation (I+N'), which has been obtained by Onsager theory(Onsager, 1949) and Flory's lattice theory(Flory, 1956; 1979). At the low temperatures of the NIT line (red line) of liquid crystals, we have a nematic (N) phase, where liquid crystals are in a nematic state but nanotubes are in an isotropic state. We predict the chimney type phase diagram with a triple point (N+I+N'). Below the triple point, we have the broad nematic-nematic (N+N') phase separation. The nematic N phase at lower concentrations consists of almost pure liquid crystals and the N' phase are formed by the orientational ordering of rods. Near $T/T_{NI}^\circ < 1$, we have the N+I phase separation.

Figure 6(b) shows the phase diagram for $c_{12} = 0.3$. On increasing the coupling constant c_{12}, the NIT lines shift to higher temperatures and lower concentrations and two NIT curves appeared in Fig. 6(a) merge. Below the NIT line (blue dotted line), we have a nematic N_0 phase, where the rods and the liquid crystals are oriented to be parallel to each other ($S_1 > 0$ and $S_2 > 0$). The width of the biphasic region I+N_0' decreases with decreasing temperature. We find the triple point (N_0+I+N_0'), where the nematic N_0, isotropic(I), and nematic N_0' phases simultaneously coexist. The binodal line of the N_0 phase shifts to higher concentrations and that of the N_0' phase shifts to lower concentrations with increasing c_{12}. Below the triple point we have the phase separation N_0+N_0', where the two nematic N_0 phases with the different concentrations can coexist.

Figure 6(c) shows the phase diagram for $c_{12} = 0.4$. The binodal curve sprits into two parts: one is the phase separation I+N_0 with the lower critical solution temperature (LCST) at $T/T_{NI}^\circ = 1$ and the other is the phase separation N_0+N_0' with the upper critical solution temperature (UCST). We have the stable nematic N_0 phase between the LCST and UCST. The length of a nanotube is also important to understand the phase diagrams. On increasing the length of the nanotube, the biphasic regions are broadened. Such LCST type phase diagram has been observed in mixtures of a main-chain nematic polyesters (poly[oxy(chloro-1,4-phenylene)oxycarbonyl][(trifluoromethyl)-1,4-phenylene]carbonyl)(PTFC) with a nematic liquid crystal (p-azoxyanisole)(PAAd14)(Ratto et.al., 1991). The theory can qualitatively describe the observed phase diagram.

3.3.2 Uniaxial nematic N_1 and N_2 phases

When the coupling parameter c_{12} is negative, we can expect that the nanotubes and liquid crystals are oriented to be perpendicular with each other.

Figure 7 shows the phase diagram for $c_{12} = -0.2(a)$ and $c_{12} = -0.5(b)$. The binodal line (solid line) is similar to Fig. 6(a), however, the structure of the nematic phases is different. In Fig. 7(a), the red dotted line at low concentrations shows the first-order nematic (N_1)-isotropic phase transition (1st-N_1IT) and the red dotted line at high concentrations shows the first-order nematic N_1-N_2 phase transition (N_1N_2T). The blue broken line corresponds to the second-order N_1-I phase transition (2nd-N_1IT), where the orientational order parameters continuously change. We also find the tricritical point (TCP) at which the 1st-N_1IT meets the 2nd-N_1IT. The phase diagram shows the three phase coexistence between N_1, I and N_2 phases at $T/T_{NI}^\circ \approx 0.92$. Above the triple point, the I+N_2 and N_1+I phase separations appear. Below the triple point, we have the N_1+N_2 phase separation.

On decreasing $c_{12}(< 0)$, the system favors more perpendicular alignment. Figure 7(b) shows the phase diagram for $c_{12} = -0.5$. (Note that the phase diagram is only shown for low

concentrations.) The two nematic-isotropic phase transitions: 1st-N_1IT and 2nd-N_1IT, shift to higher temperatures and pass the binodal line of the isotropic phase in Fig. 7(a). The 2nd-N_1IT (blue broken line) appears at lower concentrations than the binodal line and we have the homogeneous N_1 phase. Near $T/T_{NI}^\circ = 1$, the narrow biphasic region N_1+I appears. Inside the binodal region, we have the 1st-N_1IT line (red dotted line). This N_1+I phase separation disappears at TCP. At higher concentrations, the N_1+N_2 phase separation appears. The binodal curve of the coexisting N_2 phase exists at $\phi_2 \approx 0.7$, although it is not depicted in this figure. Further decreasing $c_{12}(< 0)$, the 1st-N_1IT disappears and we have the 2nd-N_1IT and the 2nd-N_1IT temperature increases with increasing ϕ_2.

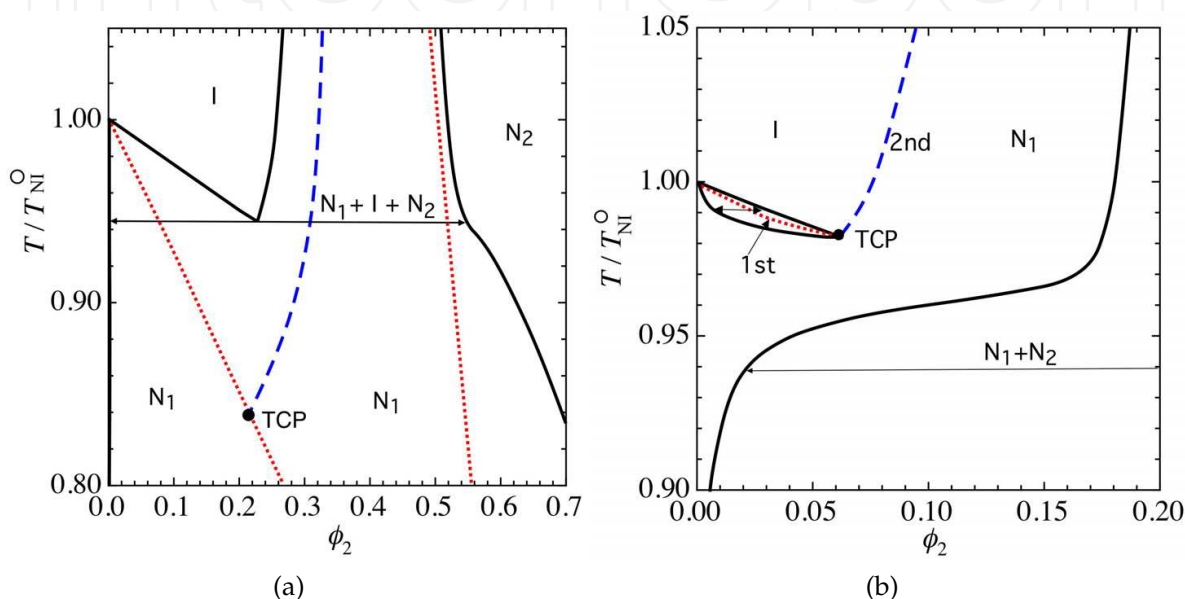Fig. 7. Phase diagrams for c_{12}=-0.2 (a) and c_{12}=-0.5 (b).

Recent experimental studies of multi-wall carbon nanotube(CNT)/nematic liquid crystal mixtures(Duran et.al., 2005) have observed the NIT temperature of the liquid crystal is enhanced by the incorporation of CNT within a small composition gap and suggested that this enhanced NIT temperature phenomenon is attributed to anisotropic alignment of liquid crystals along the CNT bundles. Our model predicts two kind of phase behavior. When the CNTs and liquid crystals are parallel, the system shows the first-order isotropic-nematic (N_0) phase transition. On the other hand, if the CNTs and liquid crystals favor to be perpendicular each other, we have the 1st- and 2nd-N_1IT. The appearance of these phase transitions is strongly effected by the orientational order of nanotubes and liquid crystals.

3.3.3 Effect of external fields

To form a nematic N_3 phase, external forces such as electric or magnetic fields will be important. When the external magnetic or electric field **E** is applied to the nanotubes and liquid crystals having a dielectric anisotropy $\Delta\epsilon_i \equiv \epsilon_{||,i} - \epsilon_{\perp,i}$ ($i = 1, 2$), the free energy changes due to the external field is given by(de Gennes & Prost, 1993)

$$a^3\beta F_{ext}/V = -\phi_1\beta\Delta\epsilon_1 \int (\mathbf{n} \cdot \mathbf{E})^2 f_1(\mathbf{u})d\Omega - \phi_2\beta\Delta\epsilon_2 \int (\mathbf{l} \cdot \mathbf{E})^2 f_2(\mathbf{u})d\Omega \qquad (33)$$

where **n** and **l** are the unit orientation vector of the liquid crystal and the nanotube, respectively.
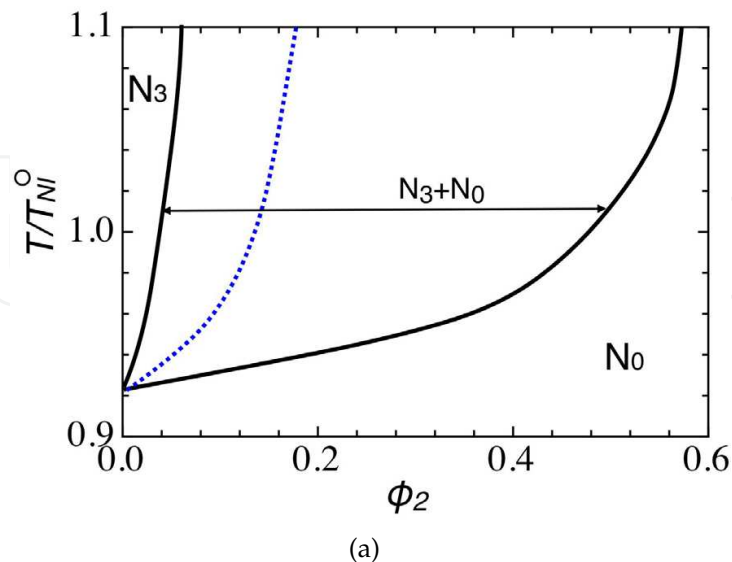

(a)

Fig. 8. Phase diagram under an external field for $\Delta\epsilon_1 = -1$ and $\Delta\epsilon_2 = 1$, where the liquid crystals tend to align perpendicular to the electric field **E**, while the nanotubes tend to parallel to **E**.
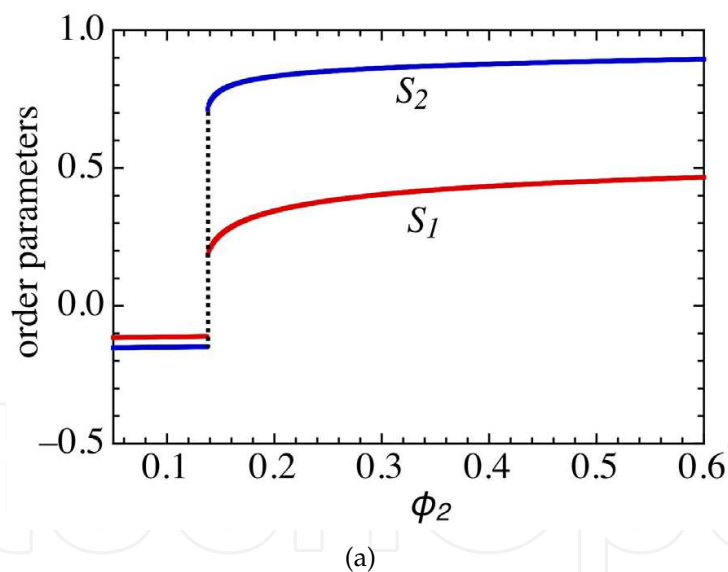

(a)

Fig. 9. Order parameters S_1 and S_2 plotted against ϕ_2 at $T/T_{NI}^\circ = 0.98$ in Fig. 8. We find the phase transition from the N$_3$ phase with $S_1 < 0$ and $S_2 < 0$ to the N$_0$ phase with $S_1 > 0$ and $S_2 > 0$.

We here consider the case of $\Delta\epsilon_1 < 0$ and $\Delta\epsilon_2 > 0$: the liquid crystals tend to align perpendicular to the electric field **E**, while the nanotubes tend to parallel to **E**. We apply the external field on Fig. 6(c), where the coupling $c_{12}(= 0.4)$ between the liquid crystal and nanotube is strong. Figure 8 shows the phase diagram under an external field for $\Delta\epsilon_1 = -1$ and $\Delta\epsilon_2 = 1$. The binodal line is broadened, compared with Fig. 6(c). We find the N$_3$ phase at low concentrations of nanotubes, where most liquid crystals tend to perpendicular

to the eternal field and nanotubes favor to be parallel to liquid crystals because of the strong coupling c_{12} even $\Delta\epsilon_2 = 1$. The blue dotted line shows the 1st-order N_3-N_0 phase transition. Figure 9 shows the order parameters plotted against ϕ_2 at $T/T_{NI}^{\circ} = 0.98$. We also find the phase separation between N_3 and N_0 phases. We emphasize that we can control the four nematic phases by applying external fields.

3.4 Biaxial nematic ordering in nanotube/liquid crystal mixtures

Biaxial nematic phase has been first theoretically predicted by Freiser(Freiser, 1970). Since then, it has been the subject of much experimental(Galerne & Marcerou, 1983; Madsen et. al., 2004; Yu & Saupe, 1980), computational(Biscarini et. al., 1995; Hudson & Larson, 1993), and theoretical(Alben, 1973; Palffy-Muhoray et. al., 1984; Sharma et. al., 1985; Straley, 1974) work (see a recent review(Tschierske & Photinos, 2010)). Biaxiality occurs if anisotropic particles orient along a second axis perpendicular to a main director of the particles(Singh, 2000). Recently it has been experimentally observed a biaxial phase in colloidal dispersions of boardlike particles(van den Pol et. al., 2009). Such biaxiality is expected significant advantages in display applications with a fast response.(Luckhurst, 2001)
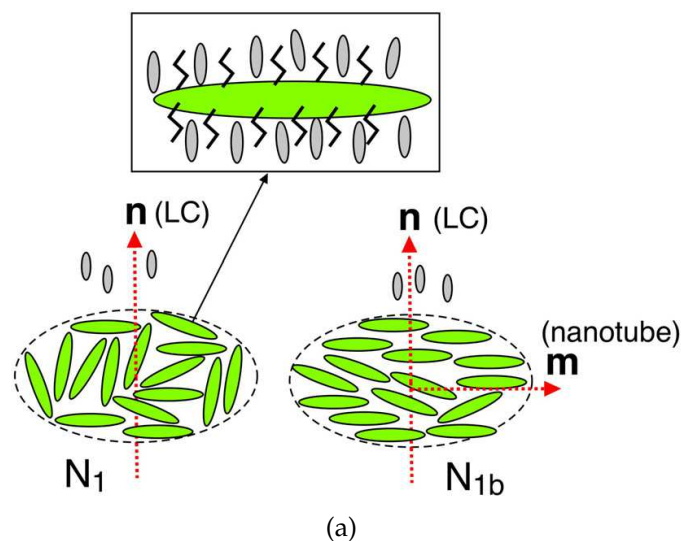

(a)

Fig. 10. Uniaxial planar nematic phase (N_1) and biaxial nematic phase (N_{1b}) in mixtures of a long nanotube and a short liquid crystal, which favor perpendicular orientations with each other. Nanotubes on an easy plane induce the additional ordering of nanotubes in the direction **m** perpendicular to the director **n** and yield a biaxial nematic phase N_{1b}.

As discussed in Section 3.1, when the order parameter of one component is positive, determining the nematic director, and the order parameter of the second component is negative, we have planar nematic phases (N_1 and N_2), where the second component is randomly distributed within the perpendicular plane to the director. In these nematic phases (N_1, N_2), we can expect either a uniaxial or a biaxial nematic phase.

Figure 10 schematically shows a novel biaxial nematic in nanotube/liquid crystal mixtures, where the two components favor a mutually perpendicular orientation.(Matsuyama, 2011) The mutually perpendicular alignments of nanotubes and liquid crystals can be achieved by wrapping polymers or surfactants on nanotube's surface(Badaire et. al., 2005; Zhang &

Kumar, 2008). To form such mutually perpendicular alignments, the anisotropic interaction (enthalpy) between a nanotube and a liquid crystal is needed. Moreover, in the planar nematic N_1 phase, on increasing concentration of nanotubes, we can expect that the excluded volume interaction (entropy) between nanotubes on an easy plane induces the additional ordering of nanotubes in the direction **m** (the second "minor" director) perpendicular to the director **n** (the first "major" director) of liquid crystals and yields a biaxial nematic phase (N_{1b}). In the N_2 phase, we may have a biaxial nematic phase (N_{2b}), where the additional ordering of liquid crystals appears in the direction **m** (minor director) perpendicular to the alignment **n** (major director) of nanotubes. Such a biaxiality in mixtures of two types of rodlike molecules has been first suggested by Alben(Alben, 1973). In this subsection, we introduce phase diagrams including such biaxial nematic phases. The phase diagrams appeared in Fig. 7 are drastically changed.

Using the distribution function $f_i(\theta, \varphi)$ of the component $i(= 1, 2)$, defined by a polar angle θ and an azimuthal angle φ, the biaxial order parameter is given by

$$\Delta_i = \int D(\theta, \varphi) f_i(\theta, \varphi) d\Omega, \tag{34}$$

where $D(\theta, \varphi) \equiv (\sqrt{3}/2) \sin^2 \theta \cos(2\varphi)$. Using the tensor order parameter

$$S_{i,\alpha\beta} = (3/2)S_i(n_\alpha n_\beta - \delta_{\alpha\beta}/3), \tag{35}$$

($\alpha, \beta = x, y, z$), we have $\Delta_i = S_{i,yy} - S_{i,xx}$ and $S_i = S_{i,zz}$(Singh, 2000). Here $S_{i,zz}$ describes alignment of molecules along the z axis (major director), whereas the nonzero value of Δ_i describes ordering along the x or y axis. Using the order parameters, we can define an isotropic (I) phase with $S_i = \Delta_i = 0$, a uniaxial N_1 phase: $S_1 > 0, S_2 < 0, \Delta_i = 0$, a uniaxial N_2 phase: $S_1 < 0, S_2 > 0, \Delta_i = 0$, a biaxial N_{1b} phase: $S_1 > 0, S_2 < 0, \Delta_i \neq 0$, and a biaxial N_{2b} phase: $S_1 < 0, S_2 > 0, \Delta_i \neq 0$. Using the additional theorem of a spherical harmonics in Eqs. (29), (30), and (31), we have $P_2(\cos \gamma) = P_2(\cos \theta)P_2(\cos \theta') + D(\theta, \varphi)D(\theta', \varphi')$ and can calculate phase separations(Matsuyama, 2011).

Figure 11 shows the phase diagrams numerically calculated for $c_{12} = -0.5$ (a) and -0.8 (b). Black lines show the binodal line. The red (blue) lines show a first (second)-order phase transition, where the order parameters discontinuously (continuously) change. The biaxial nematic phase N_{1b}, which includes an unstable biaxial phase, a metastable biaxial, and a stable biaxial phase , is indicated by the yellow area. In Fig. 11(a), at high temperatures, we have the phase separation (I+N_2) between an isotropic (I) phase at $\phi_2 \simeq 0.14$ and a uniaxial N_2 phase at $\phi_2 \simeq 0.63$. Such a chimney type's phase diagram with a coexistence between I and N phases is induced by the excluded volumes between long rods(Flory, 1956; 1979; Matsuyama & Kato, 1996; Onsager, 1949). Inside the binodal lines, we find the first-order isotropic-biaxial N_{1b} phase transition at $\phi_2 \simeq 0.22$ and the first-order biaxial N_{1b}-uniaxial N_2 phase transition at $\phi_2 \simeq 0.5$. Above $\phi_2 \simeq 0.6$, we have a stable uniaxial N_2 phase. We also find the three phase coexistence, or triple point (TP), between N_1+I+N_2 at $\tau(\equiv T/T^\circ_{NI}) \simeq 0.98$. Below the TP, we have the N_1+N_2 phase separation. At low concentrations, the N_1+I phase separation appears. The biaxial nematic phase is hidden inside the binodal lines.

Further increasing c_{12} (Fig. 11(b)), the coupling between a liquid crystal and a nanotube drastically changes the phase diagram. The biaxial regions shift to lower concentrations and
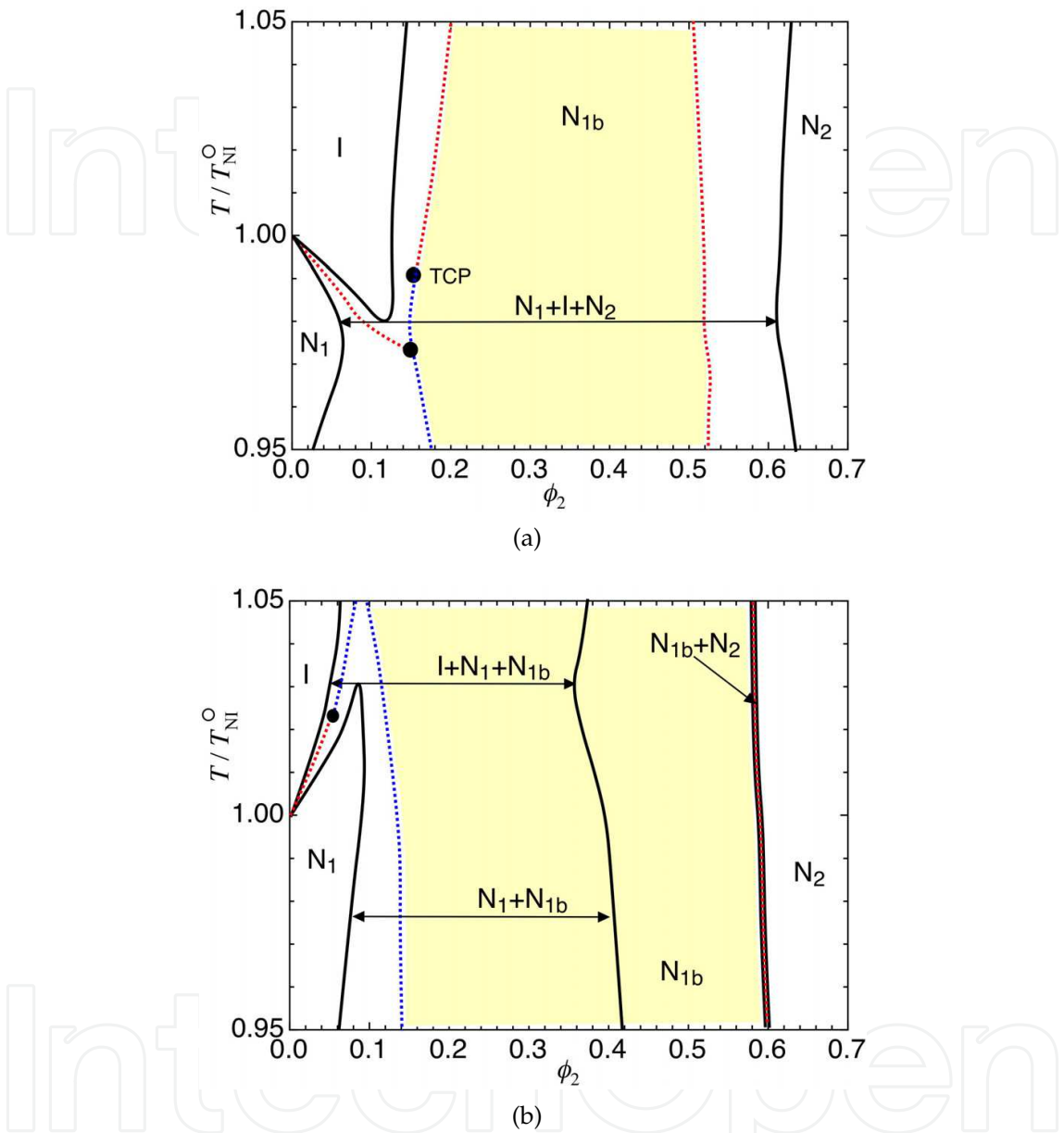
Fig. 11. Phase diagrams on the temperature ($\tau \equiv T/T_{NI}^{\circ}$)-volume fraction ($\phi_2$) plane for $c_{12} = -0.5$ (a) and -0.8 (b). The black lines indicate the binodal. The red (blue) lines show a first (second)-order phase transition, where the order parameters discontinuously (continuously) change. The biaxial nematic phase N_{1b}, which includes an unstable biaxial phase, a metastable biaxial, and a stable biaxial phase, is indicated by the yellow area. The stable biaxial phase N_{1b} appears on (b).

the thermodynamically stable biaxial N_{1b} phase appears between $\phi_2 \sim 0.4$ and $\phi_2 \sim 0.6$. We find the phase separations: $I+N_{1b}$, N_1+N_{1b}, $I+N_1$, $N_{1b}+N_2$, and the three phase coexistence $I+N_1+N_{1b}$ at $\tau \simeq 1.03$. Note that the coexistence region ($N_{1b}+N_2$) at $\phi_2 \simeq 0.6$ is very narrow. At low concentrations, the I-N_1 phase transition temperature increases with increasing ϕ_2 and the TP shifts to higher temperatures. Note that the stable biaxial phase N_{1b} appears on (b).

Duran et.al have observed in multiwall CNT/liquid crystal mixtures that the NIT temperature of the liquid crystal is enhanced by the incorporation of CNT(Duran et.al., 2005). Our theory demonstrates that this enhanced NIT temperature phenomena is attributed to anisotropic coupling between CNTs and liquid crystals. A mutually perpendicular orientation between rods and LCs can be achieved by wrapping surfactants on nanotube's surface, like a Langmuir-Blodgett film with liquid crystals(Barbero & Durand, 1996), where liquid crystals in contact with the surfactants are oriented by steric interaction with the molecules on rods. These modifications can change the strength of the interaction parameter ν_{12} in our model and give a possibility of a novel biaxial phase in this mixture. The biaxial N_{2b} phase does not appear on the phase diagrams because the length of liquid crystal is too short to form the N_{2b} phase.

4. Summary

In this chapter we have reviewed the possible phase separations in mixtures of a nanoparticle and a liquid crystal, based on the mean field theory. In Section 2, we have introduced mixtures of a spherical nanoparticle and a liquid crystal. Ferroelectric spherical nanoparticles dispersed in liquid crystal have a possibility of various phase separations, discussed in this chapter. In Section 3, we have introduced phase diagrams in mixtures of a nanotube and a liquid crystal. Novel uniaxial and biaxial nematic phases are theoretically predicted. We also discuss the effect of external fields in nanotube/liquid crystal mixtures. Phase diagrams introduced in this chapter have not been experimentally observed yet, however, it will be a challenging subject from both an experimental and theoretical point of view.

5. Acknowledgment

6. References

Alben, R. (1973).Liquid crystal phase transitions in mixtures of rodlike and platelike molecules,*J. Chem. Phys.*, Vol. 59, No. 3, (Oct. 1973) pp.4299-4304. DOI:10.1063/1.1680625.

Alder, B. J.; Wainwright, T. E. (1957). Phase Transition for a Hard Sphere System,*J. Chem. Phys.*, Vol. 27, No. 5, (Nov. 1957) pp.1208-1209. DOI:10.1063/1.1743957.

Anderson, V. J.; Terentjev, E. M.; Meeker,S.P.; Crain, J.; Poon, W. C. K. (2001). Cellular solid behaviour of liquid crystal colloids 1. Phase separation and morphology.*Eur. Phys. J. E*, Vol. 4, No. 1, (Jan. 2001) pp.11-20.

Anderson, V. J.;Terentjev, E. M. (2001). Cellular solid behaviour of liquid crystal colloids 2. Mechanical properties.*Eur. Phys. J. E*, Vol. 4, No. 1, (Jan. 2001) pp.21-28.

Araki, T.; Tanaka, H. (2004). Nematohydrodynamic Effects on the Phase Separation of a Symmetric Mixture of an Isotropic Liquid and a Liquid Crystal,*Phys. Rev. Lett.*, Vol. 93, No. 1, (Jun. 2004) pp.015702-1-015702-4. DOI:10.1103/PhysRevLett.93.015702.

Badaire, S.; Zakri, C.; Maugey, M.; Derre, A.; Barisci, J. N.; Wallace, G.; Poulin, P. (2005) Liquid Crystals of DNA-Stabilized Carbon Nanotubes,*Adv. Mater.*, Vol. 17, No. 13, (Jul. 2005) pp.1673-1676. DOI:10.1002/adma.200401741.

Barbero, G. & Durand,G. (1996). Surface Anchoring of Nematic liquid Crystals, In: *Liquid Crystals in Complex Geometries*, Crawford, G.P.; Zumer, S., (Ed.), pp.21-52, Taylor & Francis, ISBN:0-7484-0464-3, London

Basu, R.; Iannacchione, G. S. (2008) Carbon nanotube dispersed liquid crystal: A nano electromechanical system,*Appl. Phys. Lett.*, Vol. 93, No. 18, (Nov. 2008) pp.183105-1-183105-3. DOI: 10.1063/1.3005590.

Biscarini, F.; Chiccoli, C.; Pasini, P.; Semeria, F.; Zannoni, C. (1995) Phase Diagram and Orientational Order in a Biaxial Lattice Model: A Monte Carlo Study,*Phys. Rev. Lett.*, Vol. 75, No. 9, (Aug. 1995) pp.1803-1806. DOI: 10.1103/PhysRevLett.75.1803.

Brochard, F.; Jouffroy, J.; Levinson, P. (1984). Phase diagrams of mesomorphic mixtures, *J. de Phys.*, Vol. 45, No. 7, (Jul. 1984) pp.1125-1136. DOI: 10.1051/jphys:019840045070112500.

Cates, M. E.; Evans, M. R. (2000). *Soft and Fragile Matter*, Institute of Physics Publishing, ISBN: 0-7503-0724-2, Bristol.

Caggioni, M.; Giacometti, A.; Bellini, T.; Clark, N. A.; Mantegazza, F.; Maritan, A. (2005). Pretransitional behavior of a water in liquid crystal microemulsion close to the demixing transition: Evidence for intermicellar attraction mediated by paranematic fluctuations.*J. Chem. Phys.*, Vol. 122, No. 21, (Jun. 2005) pp.214721-1-214721-19. DOI:10.1063/1.1913444.

Chiu, H. W.; Kyu, T. (1999). Spatio-temporal growth of nematic domains in liquid crystal polymer mixtures.*J. Chem. Phys.*, Vol. 110, No. 12, (Mar. 1999) pp.5998-6006. DOI:10.1063/1.478502.

Copic, M.; Mertelj, A.; Buchev, O.;Reznikov, Y. (2007). Coupled director and polarization fluctuations in suspensions of ferroelectric nanoparticles in nematic liquid crystals, *Phys. Rev. E*, Vol. 76, No. 1, (Jul. 2007) pp.011702-1-011702-5. DOI:10.1103/PhysRevE.76.011702.

Courty, S.; Mine, J.; Tajbakhsh, A. R.; Terentjev, E. M. (2003). Nematic elastomers with aligned carbon nanotubes: New electromechanical actuators, *Europhys. Lett.*, Vol. 64, No. 5, (Dec. 2003) pp.654-660, DOI:10.1209/epl/i2003-00277-9.

Das, S. K.; Ray, A. D., (2005). Colloidal crystal formation via polymer-liquid-crystal demixing. *Europhys. Lett.*, Vol. 70, No. 5, (May 2005) pp.621-627. DOI: 10.1209/epl/i2005-10034-2.

de Gennes, P. G. & Prost, J. (1993). *The Physics of Liquid Crystals*, Oxford University Press, ISBN: 019-851785-8, New York.

Dierking, I.; Scalia, G.; Morales, P., (2005). Liquid crystal?carbon nanotube dispersions, *J. Appl. Phys.*, Vol. 97, No. 4, (Jan. 2005) pp.044309-1-044309-5. DOI: 10.1063/1.1850606.

Dubaut, A.; Casagrande, C.; Veyssie, M., Deloche, B., (1980). Pseudo Clearing Temperature in Binary Polymer-Nematic Solutions. *Phys. Rev. Lett.*, Vol. 45, No. 20, (Nov. 1980) pp.1645-1648. DOI:10.1103/PhysRevLett.45.1645.

Duran, H.; Gazdecki,; Yamashita, A.; Kyu, T. (2005). Effect of carbon nanotubes on phase transitions of nematic liquid crystals, *Liq. Cryst.*, Vol. 32, No. 7, (Jul. 2005) pp.815-821. DOI:10.1080/02678290500191204.

Flory, P. J. (1953). *Principles of Polymer Chemistry*, Cornell University, ISBN 0-8014-0134-8, Ithaca, New York.

Flory, P. J. (1956). Statistical Thermodynamics of Semi-Flexible Chain Molecules, *Proc. R. Soc. London Ser. A*, Vol. 234, No. 1196, (Jan. 1956) pp.60-73. DOI:10.1098/rspa.1956.0015.

Flory, P. J.; Ronca, G. (1979). Theory of Systems of Rodlike Particles: I. Athermal systems, *Mol. Cryst. Liq. Cryst.*, Vol. 54, No. 3, (Mar. 1979) pp.289-309. DOI:10.1080/00268947908084861.

Freiser, M. J. (1970). Ordered States of a Nematic Liquid, *Phys. Rev. Lett.*, Vol. 24, No. 19, (May 1970) pp.1041-1043. DOI:10.1103/PhysRevLett.24.1041.

Fukuda, J.; Yokoyama, H., (2005). Separation-Independent Attractive Force between Like Particles Mediated by Nematic-Liquid-Crystal Distortions, *Phys. Rev. Lett.*, Vol. 94, No. 14, (Apr. 2005) pp.148301-1-148301-4. DOI:10.1103/PhysRevLett.94.148301.

Fukuda, J. (2009). Liquid Crystal Colloids: A Novel Composite Material Based on Liquid Crystals, *J. Phys. Soc. Jpn.*, Vol. 78, No. 4, (Apr. 2009) pp.041003-1-041003-9. DOI: 10.1143/JPSJ.78.041003.

Galerne, Y.; Marcerou, J.P. (1983). Temperature Behavior of the Order-Parameter Invariants in the Uniaxial and Biaxial Nematic Phases of a Lyotropic Liquid Crystal, *Phys. Rev. Lett.*, Vol. 51, No. 23, (Dec. 1983) pp.2109-2112. DOI:10.1103/PhysRevLett.51.2109.

Hudson, S.D.; Larson, R.G. (1993). Monte Carlo simulation of a disclination core in nematic solutions of rodlike molecules, *Phys. Rev. Lett.*, Vol. 70, No. 19, (May 1993) pp.2916-2919. DOI:10.1103/PhysRevLett.70.2916.

Iijima, S. (1991). Helical microtubules of graphitic carbon, *Nature*, Vol. 354, No. 6348, (Nov. 1991) pp.56-58. DOI:10.1038/354056a0.

Jayalakshmi, V.; Prasad, S. K. (2009). Understanding the observation of large electrical conductivity in liquid crystal-carbon nanotube composites, *Appl. Phys. Lett.*, Vol. 94, No. 20, (May 2009) pp.202106-1-202106-3. DOI: 10.1063/1.3133352.

Kirkwood, G.; Monroe, E. (1941). Statistical Mechanics of Fusion, *J. Chem. Phys.*, Vol. 9, No. 7, (Jul. 1941) pp.514-526. DOI:10.1063/1.1750949.

Kralj, S.; Bradac, Z.; Popa-Nita, V. (2008). The influence of nanoparticles on the phase and structural ordering for nematic liquid crystals, *J. Phys.: Condens. Matter*, Vol. 20, No. 24, (Jun. 2008) pp.244112. DOI:10.1088/0953-8984/20/24/244112.

Kuksenok, O. V.; Ruhwandl, R. W.; Shiyanovskii, S. V.;, Terentjev, E. M., (1996). Director structure around a colloid particle suspended in a nematic liquid crystal, *Phys. Rev. E*, Vol. 54, No. 5, (Nov. 1996) pp.5198-5203. DOI:10.1103/PhysRevE.54.5198.

Kventsel, G. F.; Luckhurst, G. R.; Zewdie, H. B. (1985). A molecular field theory of smectic A liquid crystals, *Molc. Phys.*, Vol. 56, No. 3, (Mar. 1985) pp.589-610. DOI: 10.1080/00268978500102541.

Lagerwall, J. P. F. ; Scalia, G.; Haluska, M.; Dettlaff-Weglikowska, U.; Roth, S.; Giesselmann, F. (2007). Nanotube Alignment Using Lyotropic Liquid Crystals, *Adv. Mater.*, Vol. 19, No.3, (Feb. 2007) pp.359-364, DOI:10.1002/adma.200600889.

Li, F.; Buchnev, O.; Cheon, C.; Glushchenko, A.; Reshetnyak, V.;Reznikov, Y.; Sluckin, T. J.; West, J. L. (2006). Orientational Coupling Amplification in Ferroelectric Nematic Colloids, *Phys. Rev. Lett.*, Vol. 97, No.14, (Oct. 2006) pp.147801-1-147801-4, DOI: 10.1103/PhysRevLett.97.147801.

Li, F.; West, J.; Glushchenko, A.; Cheon, C. I.; Reznikov,Y. (2006). Ferroelectric nanoparticle/liquid-crystal colloids for display applications, *J. Soc. Info. Disp.*, Vol. 14, No. 6, (Jun. 2006), pp.523-527, DOI: 10.1889/1.2210802.

Lopatina, L. M.; Selinger, J. V. (2009). Theory of Ferroelectric Nanoparticles in Nematic Liquid Crystals. *Phys. Rev. Lett.*, Vol. 102, No.19, (May 2009) 197802-1-197802-4, DOI: 10.1103/PhysRevLett.102.197802.

Loudet, J. C.; Barois, P.; Auroy, P.; Keller, P.; Richard, H.; Pouling, P. (2004). Colloidal Structures from Bulk Demixing in Liquid Crystals, *Langmuir*, Vol. 20, No.26, (Sept. 2004) pp.11336-11347, DOI: 10.1021/la048737f.

Lubensky, T. C.; Pettey, D.; Currier, N.;Stark, H. (1998). Topological defects and interactions in nematic emulsions, *Phys. Rev. E*, Vol. 57, No.1, (Jan. 1998) pp.610-625, DOI: 10.1103/PhysRevE.57.610.

Luckhurst, G. R. (2001). Biaxial nematic liquid crystals: fact or fiction?, *Thin Solid Films*, Vol. 393, No.1, (Aug. 2001) pp.40-52, DOI: 10.1016/S0040-6090(01)01091-4.

Lynch, M. D.; Patrick, D. L. (2002). Organizing Carbon Nanotubes with Liquid Crystals, *Nano Lett.*, Vol. 2, No.11, (Nov. 2002) pp.1197-625, DOI: 10.1021/nl025694j.

Madsen, L.A.; Dingemans, T.J.; Nakata, M.; Samulski, E.T. (2004). Thermotropic Biaxial Nematic Liquid Crystals, *Phys. Rev. Lett.*, Vol. 92, No.14, (Apr. 2004) pp.145505-1-145505-4, 10.1103/PhysRevLett.92.145505.

Maier, W.; Saupe, A. (1958). A simple molecular theory of the nematic liquid-crystalline state, *Z. Naturforsch*, Vol. 13a, (Mar. 1958) pp.564-566.

Matsuyama, A. & Kato, T. (1996). Theory of binary mixtures of a flexible polymer and a liquid crystal. *J. Chem. Phys.*, Vol. 105, No.4, (Jul. 1996) pp. 1654-1660. DOI:10.1063/1.472024

Matsuyama, A.; Kato, T. (1998). Phase diagrams of polymer dispersed liquid crystals, *J. Chem. Phys.*, Vol. 108, No.5, (Feb. 1998), pp. 2067-2072, DOI: 10.1063/1.475585.

Matsuyama, A.; Evans, R. M. L.; Cates, M. E. (2000). Orientational fluctuation-induced spinodal decomposition in polymer-liquid crystal mixtures. *Phys. Rev. E*, Vol. 61, No.3, (Mar. 2000), pp. 2977-2986, DOI: 10.1103/PhysRevE.61.2977.

Matsuyama, A. (2006a). Mean Field Theory of Crystalline Ordering in Colloidal Solutions, *J. Phys. Soc. Jpn.*, Vol. 75, No.3, (Mar. 2006), pp. 034604-1-034604-9, DOI: 10.1143/JPSJ.75.034604.

Matsuyama, A. (2006b). Spinodal in a Liquid-Face Centered Cubic Phase Separation, *J. Phys. Soc. Jpn.*, Vol. 75, No.8, (Aug. 2006), pp. 084602-1-084602-10, DOI: 10.1143/JPSJ.75.084602.

Matsuyama, A. & Hirashima, R. (2008a). Phase separations in liquid crystal-colloid mixtures. *J. Chem. Phys.*, Vol. 128, No.4, (Jan. 2008) 044907-1-044907-11, DOI: 10.1063/1.2823737.

Matsuyama, A. (2008b).Morphology of spinodal decompositions in liquid crystal-colloid mixtures. *J. Chem. Phys.*, Vol. 128, No.22, (Jun. 2008) pp. (224907-1)-(224907-8), DOI: 10.1063/1.2936831.

Matsuyama, A. (2009). Phase separations in mixtures of a liquid crystal and a nanocolloidal particle. *J. Chem. Phys.*, Vol. 131, No.20, (Nov. 2009) 204904-1-204904-12, DOI: 10.1063/1.3266509.
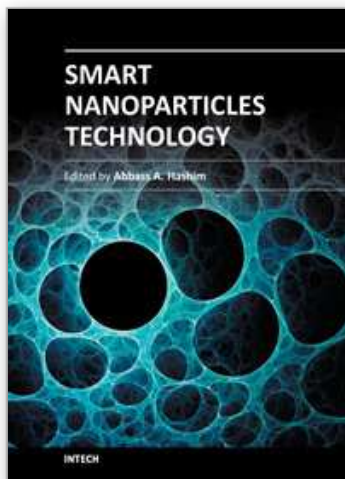
Matsuyama, A. (2010). Theory of binary mixtures of a rodlike polymer and a liquid crystal. *J. Chem. Phys.*, Vol. 132, No.21, (Jun. 2010) 214902-1-214902-10, DOI: 10.1063/1.3447892.

Matsuyama, A. (2010a). Thermodynamics of flexible and rigid rod polymer blends, In: *Encyclopedia of polymer blends, Vol. 1: Fundamentals*, Isayev, A. I., (Ed.), Chap.2, pp.45-100, WILEY-VCH Verlag GmbH & Co. KGaA, ISBN: 978-3-527-31929-9, Weinheim.

Matsuyama, A. (2011). Biaxial nematic phases in rod/liquid crystal mixtures. *Liq. Cryst.*, Vol. 38, No.6, (Jun. 2011), pp. 729-736, DOI: 10.1080/02678292.2011.570795.

Meeker,S. P.; Poon, W. C. K.; Crain, J.; Terentjev, E. M. (2000). Colloid?liquid-crystal composites: An unusual soft solid. *Phys. Rev. E*, Vol. 61, No.6, (Jun. 2000), pp.R6083-R6086, DOI: 10.1103/PhysRevE.61.R6083.

McMillan, W. L. (1971). Simple Molecular Model for the Smectic A Phase of Liquid Crystals, *Phys. Rev. A*, Vol. 4, No.3, (Sep. 1971), pp.1238-1246, DOI: 10.1103/PhysRevA.4.1238.

Musevic, I.; Skarabot, M.; Tkalec, U.; Ravnik, M.; Zummer, S. (2004). Two-Dimensional Nematic Colloidal Crystals Self-Assembled by Topological Defects. *Science*, Vol. 313, No.5789, (Aug. 2006), pp.954-958, DOI: 10.1126/science.1129660.

Nazarenko, V. G.; NychA. B.; Lev, B. I. (2001). Crystal Structure in Nematic Emulsion. *Phys. Rev. Lett.*, Vol. 87, No.7, (Jul. 2001), pp.075504-1-075504-4, DOI: 10.1103/PhysRevLett.87.075504.

Onsager, L. (1949). The Effects of Shape on The Interaction of Colloidal Particles, *Ann. N. Y. Acad. Sci.*, Vol. 51, (May 1949), pp.627-659, DOI:10.1111/j.1749-6632.1949.tb27296.x.

Palffy-Muhoray, P. ; Berlinsky, A. J.; De Bruyn, J. R.; Dunmur, D. A. (1984). Coexisting nematic phases in binary mixtures of liquid crystals, *Phys. Lett. A*, Vol. 104, No.3, (Aug. 1984), pp.159-162, DOI:10.1016/0375-9601(84)90367-0.

Popa-Nita, V.; van-der Schoot,P.; Kralj, S. (2006). Crystal Structure in Nematic Emulsion. *Eur. Phys. J. E*, Vol. 21, No.3, (Nov. 2006), pp.189-198, DOI:10.1140/epje/i2006-10059-3.

Pouling, P.; Stark, H.; Lubensky, T. C.; Weitz, D. A. (1997). Novel Colloidal Interactions in Anisotropic Fluids, *Science*, Vol. 275, No. 5307, (Mar. 1997), pp.1770-1773, DOI: 10.1126/science.275.5307.1770.

Pouling, P.; Raghunathan, V. A.; Richetti, P.; Roux, D. J. (1994). On the dispersion of latex particles in a nematic solution. I. Experimental evidence and a simple model, *J. Phys. II* , Vol. 4, No. 9, (Sept. 1994), pp.1557-1569, DOI: 10.1051/jp2:1994217.

Pusey, P. N.; van Megen, W. (1986). Phase behaviour of concentrated suspensions of nearly hard colloidal spheres, *Nature* , Vol. 320, No. 6060, (Mar. 1986), pp.340-1569, DOI: 10.1038/320340a0.

Ratto, J. A.; Volino, F.; Blumstein, R. B. (2006). Phase behavior and order in mixtures of main-chain nematic polyesters with small molecules: a combined proton and deuterium NMR study, *Macromolecules*, Vol. 24, No. 10, (May 1991), pp.2862-2867, DOI: 10.1021/ma00010a035.

Russell, M.; Oh, S.; Larue, I.; Zhou, O.; Samulski. E. T. (2006). Alignment of nematic liquid crystals using carbon nanotube films, *Thin Solid Films*, Vol. 509, No. 1-2, (Jun. 2006), pp.53-57, DOI: 10.1016/j.tsf.2005.09.099.

Skarabot, M.; Ravnik, M.; Zumer, S.; Tkalec, U.; Poberaj, I.; Babic, D.; Musevic, I. (2008). Hierarchical self-assembly of nematic colloidal superstructures, *Phye. Rev. E*, Vol. 77, No. 6, (Jun. 2008), pp.061706-1-061706-4, DOI: 10.1103/PhysRevE.77.061706.

Shaffer, M. S. P.; Windle, A. H. (1999). Analogies between Polymer Solutions and Carbon Nanotube Dispersions, *Macromolecules*, Vol. 32, No. 20, (Oct. 1999), pp.6864-6866, DOI:10.1021/ma990095t.

Sharma, S.R.; Palffy-Muhoray, P.; Bergersen, B.; Dunmur, D.A. (1985). Stability of a biaxial phase in a binary mixture of nematic liquid crystals, *Phys. Rev. A*, Vol. 32, No. 6, (Dec. 1985), pp.3752-3755, DOI:10.1103/PhysRevA.32.3752.

Shen, C.; Kyu, T., (1995). Spinodals in a polymer dispersed liquid crystal, *J. Chem. Phys.*, Vol. 102, No. 1, (Jan. 1995), pp.556-562, DOI:10.1063/1.469435.

Singh, S., (2000). Phase transitions in liquid crystals, *Phys. Rep.*, Vol. 324, No. 2, (Feb. 2000), pp.107-269, DOI:10.1016/S0370-1573(99)00049-6.

Stark, H., (1999). Director field configurations around a spherical particle in a nematic liquid crystal, *Eur. Phys. J. B*, Vol. 10, No. 2, (Jul. 1999), pp.311-321, DOI:10.1007/s100510050860.

Stark, H., (2001). Physics of colloidal dispersions in nematic liquid crystals, *Phys. Rep.*, Vol. 351, No. 6, (Oct. 2001), pp.387-474, DOI:10.1016/S0370-1573(00)00144-7.

Straley, J.P., (1974). Ordered phases of a liquid of biaxial particles, *Phys. Rev. A*, Vol. 10, No. 5, (Nov. 1974), pp.1881-1887, DOI:10.1103/PhysRevA.10.1881.

Song, W.; Kinloch, I. A.; Windle, A. H. (2003). Nematic Liquid Crystallinity of Multiwall Carbon Nanotubes, *Science*, Vol. 302, No. 5649, (Nov. 2003), pp.1363, DOI:10.1126/science.1089764.

Schymura, S.; Enz, E.; Roth, S.; Scalia, G.; Lagerwall, J. P. F. (2009). Macroscopic-scale carbon nanotube alignment via self-assembly in lyotropic liquid crystals, *Synth. Mater.*, Vol. 159, No. 21, (Nov. 2009), pp.2177-2179, DOI:10.1016/j.synthmet.2009.08.021.

Tanaka, S.; Ataka, M.; Ito, K. (2002). Pattern formation and coarsening during metastable phase separation in lysozyme solutions, *Phys. Rev. E*, Vol. 65, No. 5, (May 2020), pp.051804-1-051804-6, DOI:10.1103/PhysRevE.65.051804.

Tschierske, C.; Photinos, D.J. (2010). Biaxial nematic phases, *J. Mater. Chem.*, Vol. 20, No. 21, (Apr. 2010), pp.4263-4294, DOI:10.1039/B924810B.

van den Pol, E.; Petukhov, A.V.; Thies-Weesie, D.M.E.; Byelov, D.V.; Vroege, G.J. (2009). Experimental Realization of Biaxial Liquid Crystal Phases in Colloidal Dispersions of Boardlike Particles. *Phys. Rev. Lett.*, Vol. 103, No.25, (Dec. 2009), pp.258301-1-258301-4, DOI:10.1103/PhysRevLett.103.258301.

Weiss, V.; Thiruvengadathan, R.; Regev, O. (2006). Preparation and Characterization of a Carbon Nanotube¿Lyotropic Liquid Crystal Composite, *Langmure*, Vol. 22, No. 3, (Jan. 2006), pp.854-856, 10.1021/la052746m.

Woltman, S. J.; Jay, G. D.; Crawdord, G. P. (Eds.) (2007). *Liquid Crystals*, World Scientific Publishing, ISBN: 10-981-270-545-7, Singapore.

Yada, M.; Yamamoto, J.; Yokoyama, H., (2004). Direct Observation of Anisotropic Interparticle Forces in Nematic Colloids with Optical Tweezers, *Phys. Rev. Lett.*, Vol. 92, No. 18, (May 2004), pp.185501-1-185501-4, DOI:10.1103/PhysRevLett.92.185501.

Yamamoto, J.; Tanaka, H., (2001). Transparent nematic phase in a liquid-crystal-based microemulsion, *Nature*, Vol. 409, (Jan. 2001), pp.321-325, DOI:10.1038/35053035.

Yamamoto, R. (2001). Simulating Particle Dispersions in Nematic Liquid-Crystal Solvents, *Phys. Rev. Lett.*, Vol. 87, No. 7, (Jul. 2001), pp.075502-1-075502-4, DOI:10.1103/PhysRevLett.87.075502.

Yu, L. J.; Saupe, A. (1980). Observation of a Biaxial Nematic Phase in Potassium Laurate-1-Decanol-Water Mixtures, *Phys. Rev. Lett.*, Vol. 45, No. 12, (Sept. 1980), pp.1000–1003, DOI:10.1103/PhysRevLett.45.1000.

Zapotocky, M.; Ramos, L.; Pouling, P.; Lubensky, T. C.; Weitz, D. A., (1999). Particle-Stabilized Defect Gel in Cholesteric Liquid Crystals, *Science*, Vol. 283, No. 5399, (Jan. 1999), pp.209-212, DOI: 10.1126/science.283.5399.209.

Zhang, S.; Kinloch, I. A.; Windle, A. H. (2006). Mesogenicity Drives Fractionation in Lyotropic Aqueous Suspensions of Multiwall Carbon Nanotubes, *Nano Lett.*, Vol. 6, No. 3, (Mar. 2006), pp.568-572, DOI: 10.1021/nl0521322.

Zhang, S.; Kumar, S. (2008). Carbon Nanotubes as Liquid Crystals, *Small*, Vol. 4, No. 9, (Sep. 2008), pp.1270-1283, 10.1002/smll.200700082.

Smart Nanoparticles Technology

Edited by Dr. Abbass Hashim

In the last few years, Nanoparticles and their applications dramatically diverted science in the direction of brand new philosophy. The properties of many conventional materials changed when formed from nanoparticles. Nanoparticles have a greater surface area per weight than larger particles which causes them to be more reactive and effective than other molecules. In this book, we (InTech publisher, editor and authors) have invested a lot of effort to include 25 most advanced technology chapters. The book is organised into three well-heeled parts. We would like to invite all Nanotechnology scientists to read and share the knowledge and contents of this book.

How to reference

In order to correctly reference this scholarly work, feel free to copy and paste the following:

Akihiko Matsuyama (2012). Phase Separations in Mixtures of a Nanoparticle and a Liquid Crystal, Smart Nanoparticles Technology, Dr. Abbass Hashim (Ed.), ISBN: 978-953-51-0500-8, InTech, Available from: http://www.intechopen.com/books/smart-nanoparticles-technology/phase-separations-in-mixtures-of-a-nanoparticle-and-a-liquid-crystal

INTECH
open science | open minds